




## Article

# Interdisciplinary Analysis and the Role of Experiments in Raw Materials and Technology Identification for Prehistoric Pottery in the Bistrița River Basin (Romania)

Ana Drob <sup>1</sup>, Neculai Bolohan <sup>2</sup>, Viorica Vasilache <sup>1,\*</sup>, Bogdan-Gabriel Rățoi <sup>3</sup> and Mihai Brebu <sup>4</sup>

<sup>1</sup> Arheoinvest Centre, Department of Exact Sciences and Natural Sciences, The Institute of Interdisciplinary Research, “Alexandru Ioan Cuza” University of Iași, 700506 Iași, Romania; ana.drob@uaic.ro

<sup>2</sup> Faculty of History, “Alexandru Ioan Cuza” University of Iași, 700506 Iași, Romania; neculaibolohan@yahoo.com

<sup>3</sup> Faculty of Geography and Geology, “Alexandru Ioan Cuza” University of Iași, 700505 Iași, Romania; bog21rat@gmail.com

<sup>4</sup> Laboratory of Physical Chemistry of Polymers, Institute of Macromolecular Chemistry “Petru Poni” Iași, 700487 Iași, Romania; bmihai@icmpp.ro

\* Correspondence: viorica\_18v@yahoo.com or viorica.vasilache@uaic.ro

**Abstract:** The paper presents an interdisciplinary study based on an experimental model for investigating clay sources to identify prehistoric human behavior regarding resources. The study focuses on the Middle Bronze Age (1955/1773–1739/1614 cal. BC) settlement of Silișteea-*Pe Cetățuie* in eastern Romania, where archaeological materials from the Costișa and Monteoru cultures were discovered. Standard criteria for macroscopic analysis and analytical techniques, such as optical microscopy (OM), Scanning Electron Microscopy with Energy Dispersive X-ray Spectroscopy (SEM-EDX), Micro-Fourier Transform Infrared Spectroscopy ( $\mu$ -FTIR), and thermal analysis (DTA and TG), were used to investigate the ceramic material from multiple points of view. The results showed that there were no significant differences between the ceramics of the two communities. Putting together the data obtained from macroscopic and physico-chemical analyses helped in partially reconstructing ancient human behaviors related to the production and use of ceramic vessels.

**Keywords:** interdisciplinary; clay; sources; experiment; Middle Bronze Age; eastern Romania



**Citation:** Drob, A.; Bolohan, N.; Vasilache, V.; Rățoi, B.-G.; Brebu, M. Interdisciplinary Analysis and the Role of Experiments in Raw Materials and Technology Identification for Prehistoric Pottery in the Bistrița River Basin (Romania). *Heritage* 2024, 7, 5120–5147. <https://doi.org/10.3390/heritage7090242>

Academic Editors: Silvano Mignardi, Nikolaos Laskaris, Lamprini Malletzidou, Anastasia Rousaki and Georgios S. Polymeris

Received: 11 June 2024

Revised: 10 September 2024

Accepted: 11 September 2024

Published: 13 September 2024



**Copyright:** © 2024 by the authors. Licensee MDPI, Basel, Switzerland. This article is an open access article distributed under the terms and conditions of the Creative Commons Attribution (CC BY) license (<https://creativecommons.org/licenses/by/4.0/>).

## 1. Introduction

The ceramic fragments discovered in archaeological excavations represent an important clue in establishing the nature of the relationships between the cultures of communities from different historical periods. The specific pottery of these communities can be studied to identify their behavior in terms of similarities or differences regarding ceramic processing technology, raw material sources, and functionality.

Applying a wide range of criteria and complementary theoretical approaches to the interpretation of pottery offers a broader perspective on the factors involved in its production, use, and abandonment. Thus, ceramic ecology and functionalism significantly contribute to the study of pottery, enabling us to transcend traditional cultural perspectives that primarily concentrate on the typological classification of ceramics, a concept that requires an understanding of archaeological historicity. Furthermore, both approaches emphasize the development of a coherent methodology for the study of pottery, which involves the use of multiple archaeometric techniques that allow for an in-depth study of ceramic materials and their properties. In addition to the elements derived from these two approaches, the social perspective involves integrating individuals as active participants in the production and use of pottery, thus contributing to its interpretation.

To create the experimental model, it is necessary to understand aspects related to the origin of clays as well as natural clay deposits and their processing methods for pottery

making. Researchers have identified several models regarding the source of clay raw materials, both ethnographically and experimentally: 1. The term “areal” refers to the supply area, which assumes the existence of large cultural or geographical “super-groups” as the production area; 2. Regional factors include supply regions, cultural and geographical groups, and the production region itself; 3. Zonal supply zones, as well as zonal cultural and geographical formations, constitute the production zone; 4. Territorial production includes local and small cultural groups; 5. Local workshop refers to the site level and includes immediate sources [1].

Regarding clay deposits, they are generally represented by “clay pits”, places from which clay is extracted and still used today for various purposes. Furthermore, alluvial clay serves as a significant resource that finds application in diverse settings. However, accessibility, along with its qualities and properties, largely determines the location of clay extraction. After identifying a potential source, a specific quantity was extracted and processed in the laboratory to carry out the experimental study [2].

Two studies in Romania focus on identifying the raw material sources used in pre-history through physico-chemical analyses [3,4], while numerous experimental studies at the international level [1,2,5–7] demonstrate the significance of these investigations and the effectiveness of the interdisciplinary approach through verifiable results. The interdisciplinary approach outlined highlights the intricate relationships between natural sciences and archaeology, particularly in the identification of clay sources used in pottery production. This complex field not only helps to determine the technological aspects of ancient ceramic production but also provides valuable insights into the socio-economic and cultural dynamics of past societies. Based on some of the most recent studies, the following is a broader contextualization:

#### 1. Cultural and technological considerations in clay procurement.

The identification of clay sources goes beyond geology, as emphasized by Gliozzo, 2020 [1]. It involves understanding the choices made by ancient communities regarding the materials they used, which often reflect cultural preferences, economic strategies, or technological advancements. These choices reveal how societies accessed and utilized local or distant resources, potentially linked to trade networks or territorial control. The recognition of preferred clay types indicates both environmental availability and cultural significance, where certain clay types may have been associated with specific traditions or technological processes.

#### 2. Assessing technological suitability and supply basins

Montana, 2020 [2] and Gualtieri, 2020 [5] emphasize the role of mineralogical and petrographic analysis in identifying raw materials. Ancient potters not only determined the technological suitability of a particular clay by its physical properties but also by their knowledge about its treatment, such as the need for specific tempering or firing techniques. Archaeologists can infer from these findings whether ancient societies sourced the clay locally or imported it from afar, which sheds light on mobility, trade, and the logistical challenges they faced in procuring and transporting these materials. Such investigations also indicate the existence of “supply basins”, regions central to pottery production or distribution, contributing to a broader understanding of regional interactions.

#### 3. Chemical analyses and provenance studies

The application of chemical analysis techniques, as discussed by Hein and Kilikoglou, 2020 [6], is crucial for identifying the elemental composition of clay and its geographic origin. Spectrometric methods allow for precise fingerprinting of clay sources. This helps map ancient trade routes and patterns of resource distribution, revealing connections between distant regions. Provenance studies are particularly valuable for examining the exchange of goods and the spread of technological innovations across cultures. By linking a particular ceramic type to its clay source, archaeologists can trace the flow of materials and ideas.

#### 4. Cultural continuities and technological conservatism

The research by Koutouvaki et al., 2021 [4] on pottery from the Chalcolithic site of Radovanu (Romania) highlights the role of shared traditions and conservatism in pottery production. Analysis of ceramic fragments from technological and stylistic perspectives can reveal cultural and technical continuities across generations. In this context, identifying clay sources becomes not just a matter of resource management but also a component of cultural identity.

#### 5. Impact of clay source studies on socio-economic understanding

The identification of clay sources contributes to a more detailed reconstruction of past socio-economic dynamics. By pinpointing supply basins and technologies used in ceramic production, archaeologists gain a deeper understanding of the complexity of interactions between communities, the nature of trade relations, and cultural exchanges. Furthermore, the study of raw materials can reveal information about technological specialization in certain regions and suggest the existence of production centers.

In archaeology, the identification of clay sources is a complex and interdisciplinary field of research that combines advanced methods from the natural sciences with archaeological insights into ancient technology and economy. The recent references provided in this context reflect the breadth and variety of approaches used in this field of research.

Thus, based on knowledge and the know-how used in these studies, this research seeks to expand the narratives about the prehistoric communities in the Eastern Carpathian area by obtaining special data that meet international research standards and increasing the number of case studies.

Our study focused on two sets of 24 ceramic fragments from the Costișa and Monteoru cultures found at the Siliștea-Pe Cetățuie site in eastern Romania, as well as four types of clay from the nearby area that could serve as potential raw material sources. In this regard, a comparative approach and an experimental model were used, with the study's main objective being to identify the raw material source used by these two communities in the Middle Bronze Age. The analysis involved optical microscopy (OM), Scanning Electron Microscopy with Energy Dispersive X-ray Spectroscopy (SEM-EDX), Micro-Fourier Transform Infrared Spectroscopy ( $\mu$ -FTIR), and thermal analysis.

## 2. Materials and Methods

### 2.1. The Archaeological Context and Discoveries from the Siliștea-Pe Cetățuie Settlement

The Siliștea-Pe Cetățuie site is located at the southeastern extremity of the Cracău-Bistrița Depression in the Siliștea village (Români commune, Neamț County; GPS: N 46°47'43.81"; E 26°43'33.00"). The settlement is situated in a high area with good visibility, located in a wide convergence area of the Bistrița River with the Siret River, both waterways being important communication routes in the Eastern Carpathian region. Only one habitation level has been identified in the fortified settlement where archaeological materials from the Costișa and Monteoru cultures were discovered and are not stratigraphically differentiated [8–10].

The Cetățuia plateau at Siliștea is 448.66 m high and has an NNV-SSE orientation. Steep slopes with an inclination of 25–37° naturally defend the settlement from three directions (N, E, and W), creating accessibility difficulties [11,12]. The defensive system was supplemented by an anthropic ditch with a depth of 3.20 m and an opening of 15 m, which was lined with sandstones from the hill's geological structure, an aspect considered a novelty in the construction of such structures [10]. Geologically, the settlement plateau contains Quaternary deposits from the Middle Pleistocene, consisting of sands, gravel, pebbles, and loessoid deposits. Near the site, there are Neogene sedimentary deposits consisting of sands, marly clays (marl or marlstone is a carbonate-rich mud or mudstone, which contains variable amounts of clays and silt), rock salt, gypsum, and tuff (tuff composed of sandy volcanic material can be referred to as volcanic sandstone). Pedologically, both in the settlement area and in its proximity, there are acidic brown soils with low fertility, often used as pastures and hayfields.

From the excavations carried out over time (2000–2021), a rich archaeological material has emerged, including bone artifacts (awls, pendants, arrowheads), stone artifacts (axes, curved knives, arrowheads, grinding stones), clay artifacts (spindle whorls), metal artifacts (six *Noppenringe* hair rings, a simple ring, a bracelet, and a small ring), and fragments of pottery specific to the Costișa and Monteoru cultures, originating from various types of vessels (storage, cooking, ornamental, etc.).

## 2.2. Materials and Sample Preparation Methodology

The study analyzed 24 ceramic fragments from the Costișa culture (labeled C1–C24) and 24 from the Monteoru culture (labeled M1–M24). Also, the statistical representation of the functional classes was considered when choosing the number of samples for analysis. Thus, the attempt was to maintain proportions, but on a reduced scale, by selecting a representative number of ceramic fragments from each functional category.

The macroscopic analysis of the pottery from the two ceramic groups from the Silișteea-Pe Cetățuie settlement revealed several common features associated with the production of pottery from this site. Thus, it was established that all the vessels were made using the coiling technique, which was identified by the fine unevenness on the inner surfaces or by the joining marks on the edges of the ceramic fragments. The auxiliary elements (handle, grippers) that appear on some containers were made by modeling, with the traces of their joining and finishing being visible most of the time.

The vessels' outer and inner surfaces are generally very well finished, with no traces of polish. In certain instances, the exterior of both pottery assemblages displays a treatment known as ceramic slip. Also, the vessels from the functional categories of cooking and preparation, serving, and consumption present traces of smoking that are visible on the inside, as well as spots of secondary burning on the outside that have penetrated the wall of the container. These are indications of the use of containers when preparing hot food.

The colors and shades of the vessels are mostly different, but in the case of Costișa, they seem to be more unified. The chromatic variety of the containers may indicate a poorly controlled firing that does not allow for obtaining homogeneous colors. The lack of a correlation between vessel type and color in any functional class of pottery, including Costișa and Monteoru, suggests a common firing process for all containers without any preference for specific treatments.

In all the fragments studied, ceramoclasts are present as intentional inclusions, and three types of paste for the pottery of both communities have been identified and differentiated based on their quantity, shape, and distribution. Regarding the Costișa pottery, the first category identifies a paste containing small, rounded ceramoclasts with a reduced distribution of 5–10%, used in the creation of vessels serving various special and multipurpose functions. The second category includes medium-sized, sub-rounded, and sub-angular ceramoclasts, which have a frequency of 10–15% and are found in the paste of cooking vessels and those for transporting and storing liquids. The third category is characterized by medium and large ceramoclasts, sub-rounded and sub-angular, with a distribution of 15–20%, being characteristic of vessels for preparation, serving, and consumption and those for storing solid or liquid goods. In the case of the Monteoru pottery, the first category includes small, rounded ceramoclasts, which have a distribution of 5–10% and are characteristic of vessels with multiple destinations. The second category includes medium, sub-rounded, and sub-angular ceramoclasts, with a frequency of 10–15%, which are used to make cooking vessels, preparation, serving, and consumption, as well as transportation and liquid storage. The third category of paste is characterized by medium and large ceramoclasts, sub-rounded and sub-angular, with a frequency of 15–20%, specific to storage vessels.

To confirm the EDX results,  $\mu$ -FTIR showed that carbonates were present in almost all the samples, though post-depositional processes may have been involved, pointing to a firing temperature lower than 700–750 °C. In addition, in the case of the Monteoru pottery, two samples were identified that were fired at temperatures lower than 500–550 °C, a spectral clue that supports low firing temperature and less post-depositional processes,

and four samples were also identified (M6, M17), which indicate conditions higher than 700–750 °C. In this sense, the statistical representation of these conditions, most likely accidental exceptions, of the way the vessels were placed in the firings does not constitute determined elements in the stability of several firing intervals.

Therefore, through EDX and  $\mu$ -FTIR analyses, the use of a local kaolinite clay with a high iron content, which presents the same mineralogical and physico-chemical characteristics, was highlighted. Regarding the pyrotechnic elements, through interdisciplinary studies, it was possible to establish that the pottery of both communities was fired, in general, at temperatures between 500/550 °C and 700/750 °C. The varied colors of the pottery, the different firing atmospheres, and the temperatures reached in the process show that the firing of the vessels was most likely carried out in pits or above ground.

The samples for the experiment are represented by four types of clay (labeled S1–S4) from potential exploitation areas to identify the source of the raw material. Therefore, the clay pit, located approximately 250 m at the base of the western slope of the settlement, and the samples originating from the lower and intermediate levels of the clay deposit, labeled S1 and S2, represent the first source (Figure 1a). The eastern slope of the settlement, approximately 60 m from the inhabited plateau, represents the second source, represented by the clay samples labeled S3 and S4 (Figure 1b).



**Figure 1.** Map showing the clay samples used in the experiment's source areas: (a)—Sources S1 and S2 (clay deposit); (b)—Sources S3 and S4 (slope of the settlement).

The obtained clays were crushed (Figure 2(Ia)) and sieved (Figure 2(Ib)), then shaped into 3 × 3 cm squares with a thickness of 1–2 cm, and the test samples obtained were air-dried at room temperature (21 °C) for 48 h.

After drying, the test samples were fired in an oxidizing atmosphere at temperatures of 450 °C, 700 °C, and 900 °C (Figure 2(II)) in a Nabertherm furnace. These firing intervals were selected in accordance with the results from the interdisciplinary analyses performed on the ceramic fragments. Subsequently, the obtained samples were studied following the same investigation steps proposed for the pottery analysis.

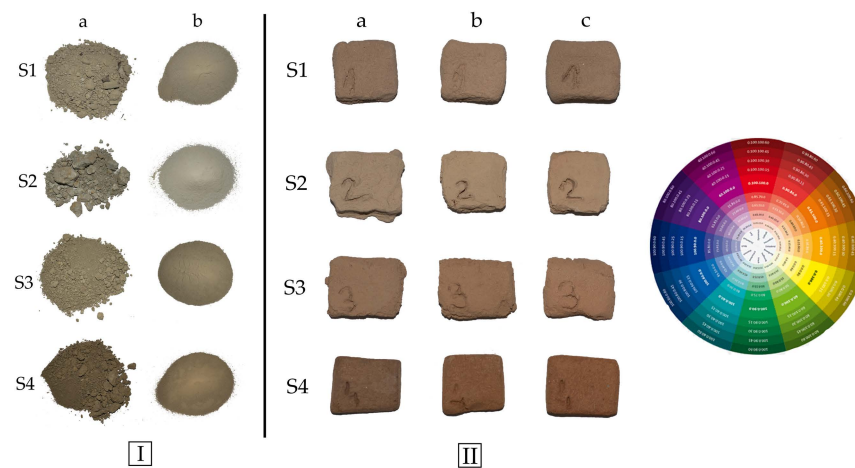


**Figure 2.** (I) The clay samples collected: (a) crushed; (b) sieved. (II) The test samples obtained after firing: (a)—450 °C; (b)—700 °C; (c)—900 °C.

### 2.3. Analytical Methods

In the microscopic analysis of the samples, a Zeiss Imager.a1M microscope with a built-in AXIOCAM camera was used, using AxionVisionRelease 4.7.1 software produced by Zeiss, Oberkochen, Germany. The samples were sanded with a Struers LaboPol device (Struers, Copenhagen, Denmark) using discs with different abrasion sizes. The mineralogical analysis was performed using cross-polarized and parallel-polarized nicoli.

In the current analyses, an electron microscope with SEM scan, model VEGA II LSH, produced by TESCAN (Brno, Czech Republic), was used, coupled with an EDX detector type QUANTAX QX2, produced by BRUKER/ROENTEC (Berlin, Germany). The SEM micrographs were obtained by backscattered electrons (BSE) at 200× magnifications for the pottery and clay samples without carbon or metal covering. The working distance was set at 16.600 mm, with an accelerating voltage of 20 kV, under vacuum conditions made with nitrogen gas.

The spectra were recorded using an FTIR spectrophotometer and HYPERION 1000 microscope, both from Bruker Optics, Germany. The FTIR spectrophotometer is of the TENSOR 27 type, which is predominantly suitable for close IR measurements. The standard detector, DLaTGS, covers the spectral range of 7500–370  $\text{cm}^{-1}$  and works at room temperature. The resolution is usually 4  $\text{cm}^{-1}$ , but it can also reach 1  $\text{cm}^{-1}$ . The detector is of the MCT type and cooled with liquid nitrogen (−196 °C), and the measured area is optimized to a diameter of 250  $\mu\text{m}$  with the possibility of reaching a minimum of 20  $\mu\text{m}$ . For the  $\mu\text{FTIR}$  investigation, the samples were analyzed without any preparation in reflectance mode with a number of 32 scans per sample at a resolution of 4  $\text{cm}^{-1}$ . The specific peaks were identified for each spectrum and then superimposed for a comparative view even though quality and details are not visible.

The DTA and TG curves were recorded simultaneously using a Linseis STA PT-1600 (Linseis, Selb, Germany) at a heating rate of 10 °C/min in a dynamic air atmosphere with a flow rate of 50 mL/min to simulate real conditions during the thermal decomposition of the samples. The device operates using specialized software. The samples were weighed on an electronic balance (model: PARTNER AS220/C/2) and did not exceed 50 mg. The maximum temperature was set at 1000 °C.

## 3. Results and Discussions

### 3.1. Results and Discussions Regarding the Costișa and Monteoru Ceramic Fragments

#### 3.1.1. Microscopic Analysis

The Costișa (Figure 3) and Monteoru (Figure 4) samples underwent optical microscopy, revealing the presence of mineral inclusions like quartz, mica, and iron oxides, as well as intentional inclusions like ceramoclasts. Also, reused ceramoclasts in 13 Costișa fragments

(C1–C6, C9, C12, C13, C15, C17–C19) and 14 Monteoru fragments (M1–M3, M5, M8–M12, M14, M16, M21, and M23) were identified.

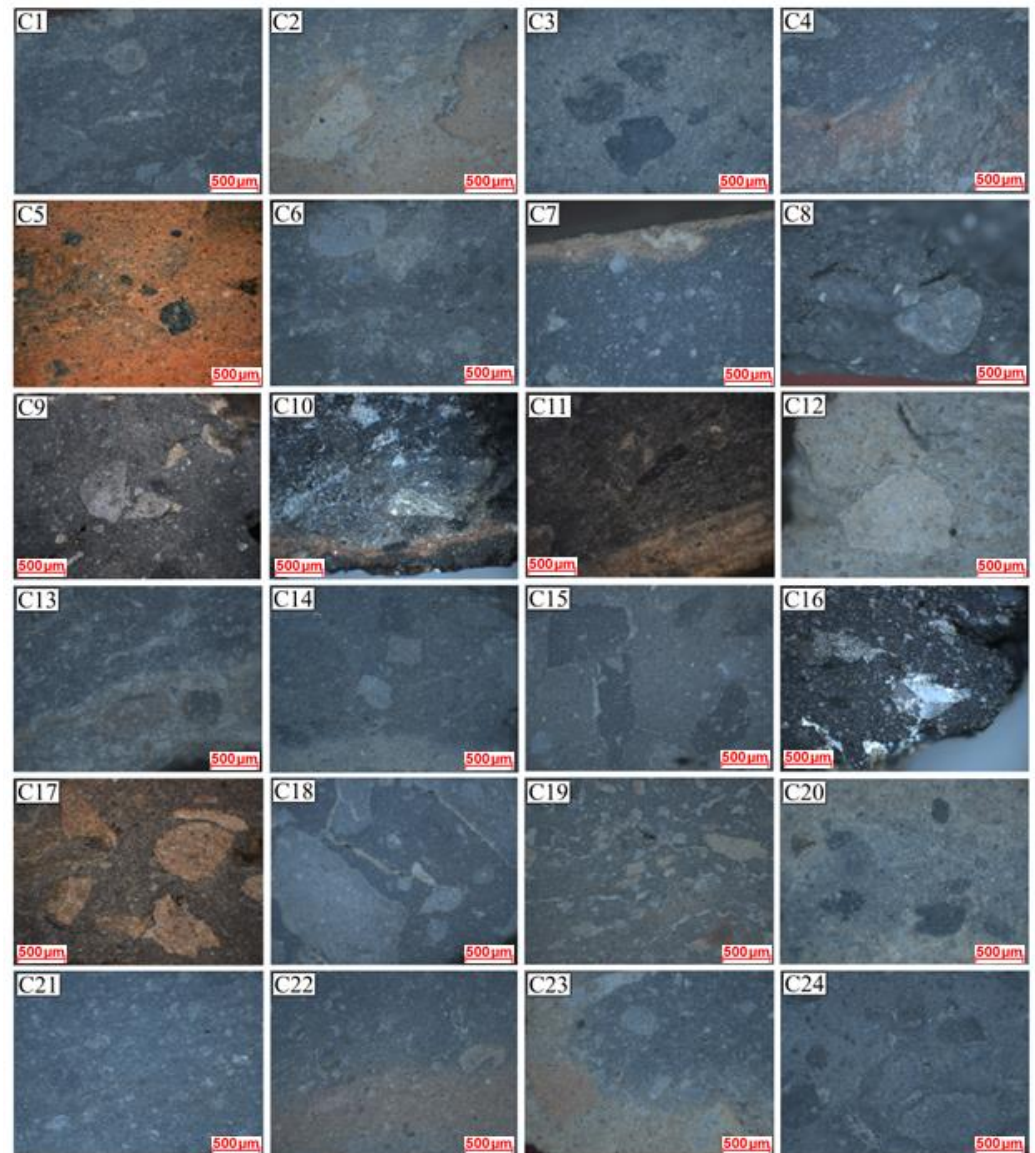


**Figure 3.** OM images of the Costișa ceramic fragments from Silișteea-Pe Cetățuie (50× magnification).

Carbonates are visible in five Costișa samples (C9, C11, C13, C16, and C18) and six Monteoru samples (M5, M6, M7, M13, M16, and M19), suggesting a low firing temperature, an aspect also confirmed by EDX and FTIR analyses [13,14]. Another indication of relatively low firing temperatures is the presence of traces of organic matter, visible as black pores or flakes, identified in six Costișa samples (C13, C14, C15, C17, C20, and C23) and six Monteoru samples (M2, M6, M9, M10, M14, and M22). Iron oxides, visible in all fragments, have appreciable dimensions or are discreetly present as other natural inclusions in the ceramic paste.

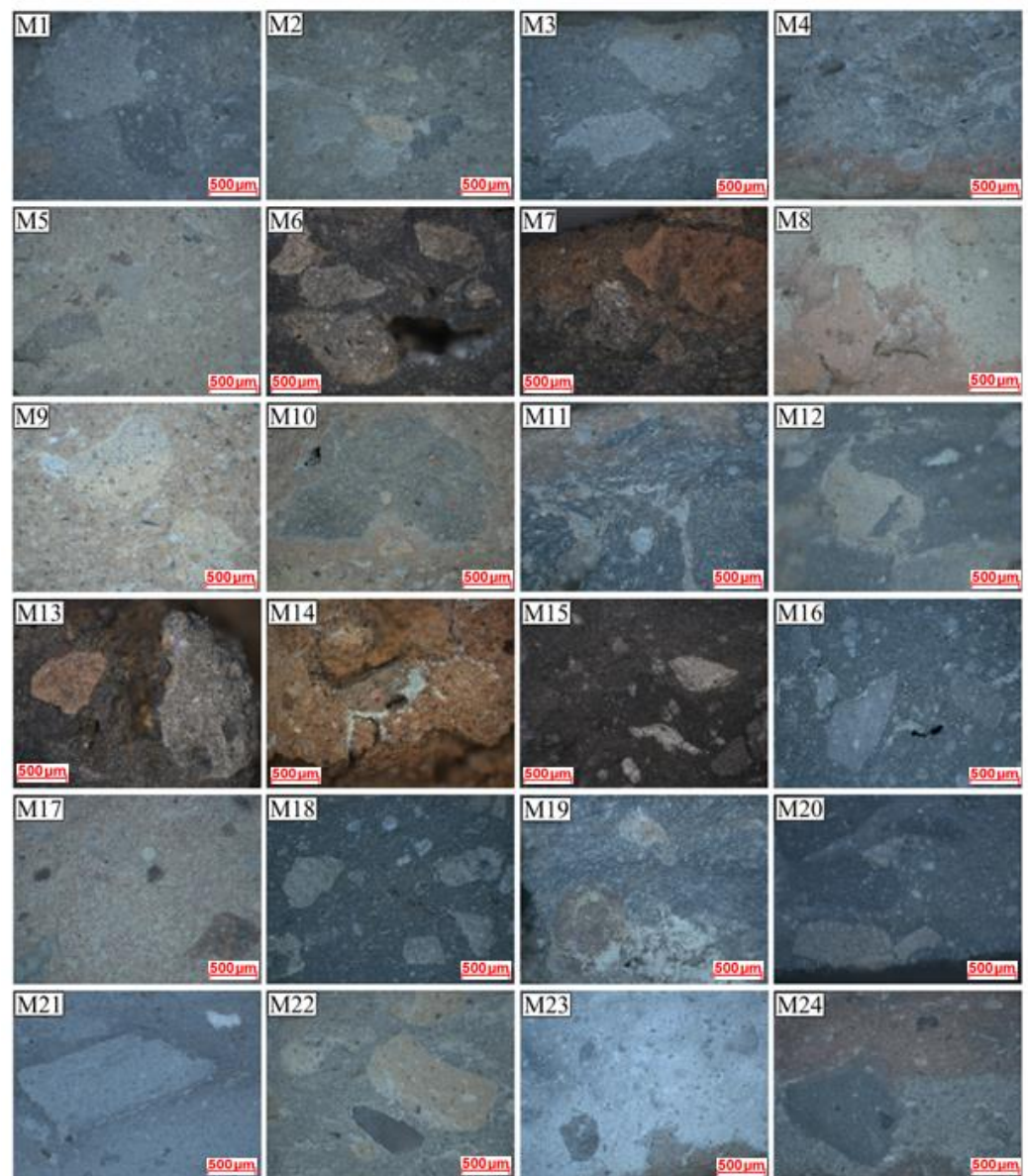


**Figure 4.** OM images of the Monteoru ceramic fragments from Siliștea-Pe Cetățuie (50× magnification).

### 3.1.2. Mineralogical Analysis

To obtain mineralogical information, four thin sections were prepared for two Costișa ceramic fragments (C9—Figure 5; C23—Figure 6) and two Monteoru fragments (M2—Figure 7; M15—Figure 8). These were analyzed under the optical microscope using cross-polarized and parallel-polarized nicoli.

For both samples, the presence of subangular monoclinic quartz crystalloclasts, as well as polycrystalline quartz crystals resulting from pottery firing, was highlighted. In addition to these, muscovite, plagioclase feldspars, and hematite aggregates were identified. Their presence is also confirmed by EDX and FTIR analyses of the clay. Furthermore, in both samples, the presence of ceramoclasts and primary pores resulting from clay kneading is noticeable. Additionally, a limestone lithoclast (C9) and a sandstone lithoclast (C23) were identified.

Following the mineralogical analysis of the four pottery fragments, a series of data regarding the clay used in the vessel's manufacture was obtained. Thus, a local sandy clay with an amorphous appearance and semi-oriented texture was used, indicating semi-fine to fine pottery with intentional inclusions like ceramoclaste.



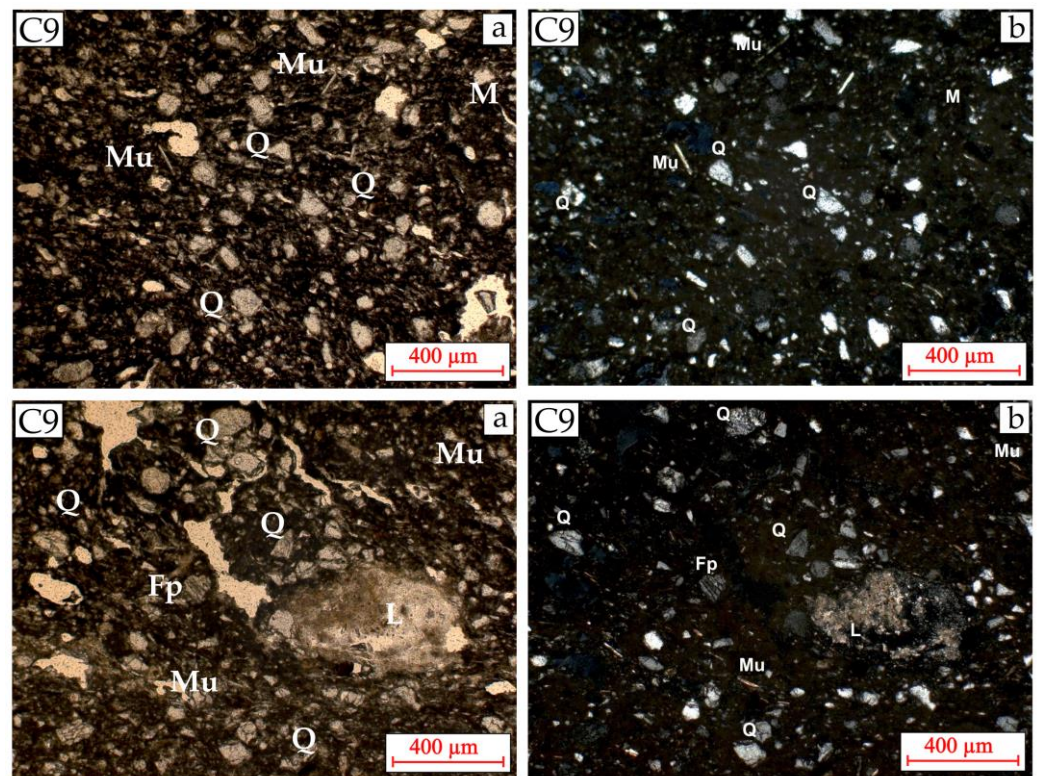


**Figure 5.** Mineralogical section of fragment C9: Q—quartz; Mu—muscovite; Fp—plagioclase feldspar; L—limestone lithoclast; M—amorphous matrix ((a)—parallel nicoli; (b)—cross nicoli).

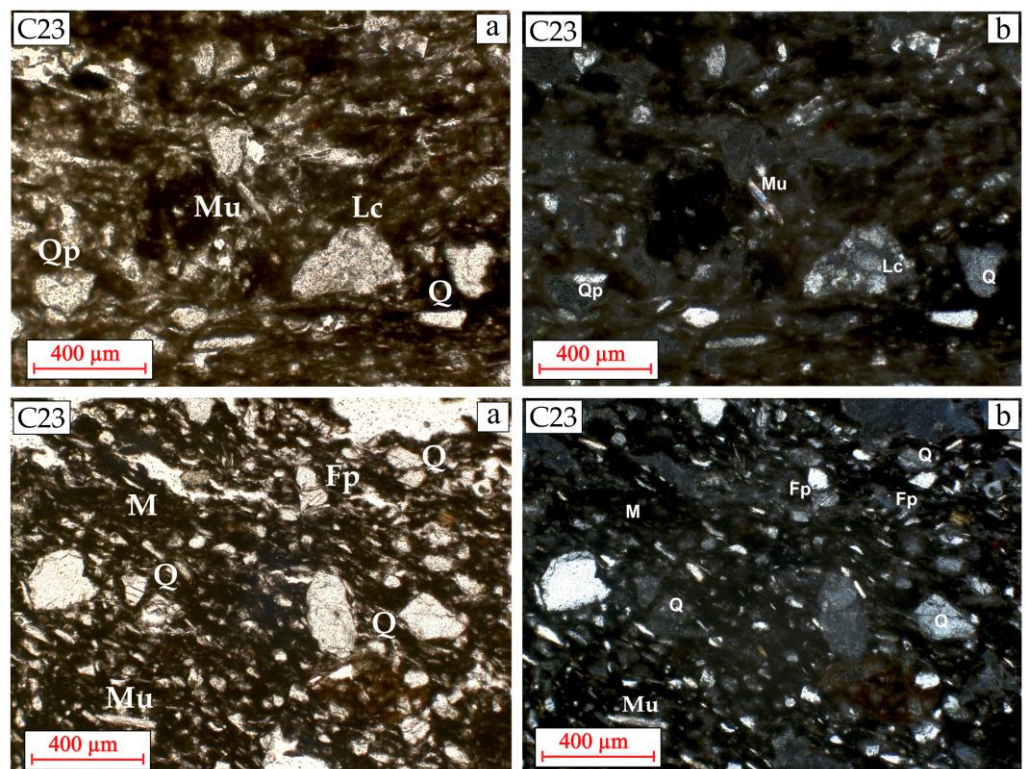


**Figure 6.** Mineralogical section of fragment C23: Q—quartz; Qp—polycrystalline quartz; Mu—muscovite; Fp—plagioclase feldspar; Lc—sandstone lithoclast; M—amorphous matrix ((a)—parallel nicoli; (b)—cross nicoli).

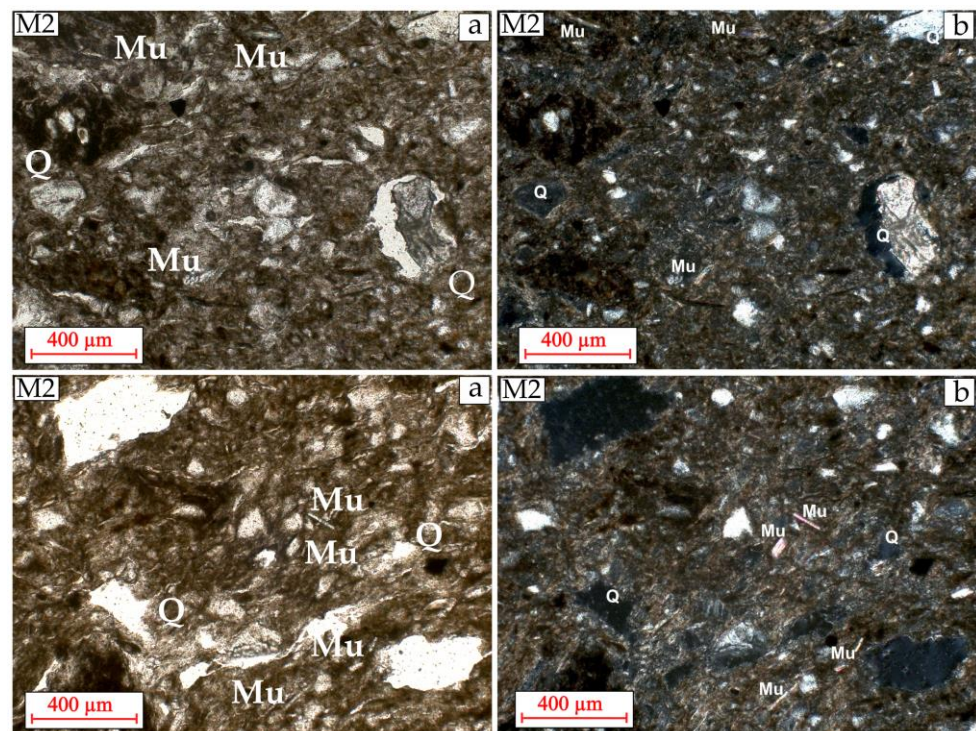


**Figure 7.** Mineralogical section of fragment M2: Q—quartz; Mu—muscovite ((a)—parallel nicoli; (b)—cross nicoli).

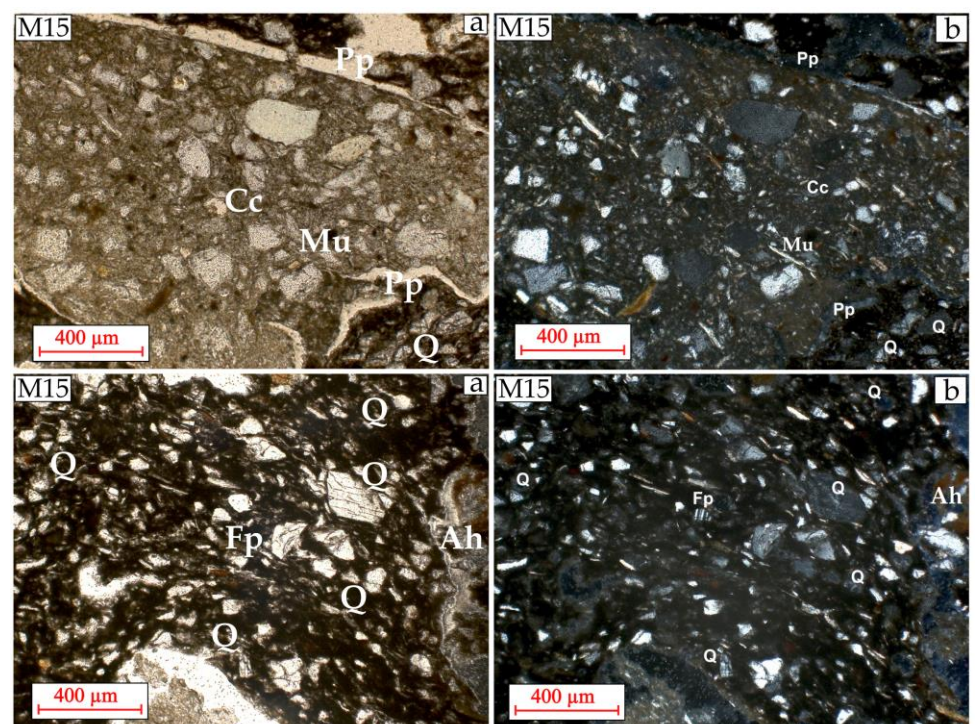


**Figure 8.** Mineralogical section of fragment M15: Q—quartz; Mu—muscovite; Ah—hematite aggregates; Cc—ceramoclaste; Fp—plagioclase feldspar; Pp—primary pores ((a)—parallel nicoli; (b)—cross nicoli).

### 3.1.3. SEM-EDX Analysis

The SEM micrographs for the Costișa pottery clay matrix illustrate good homogeneity, with microstructural elements incorporated into the clay matrix (Figure 9). In this

regard, several samples (C7, C9–C11, C13, C16, and C18) have been identified, where homogeneity is lower, with large pores and very well-individualized microgranules [15,16] are present. These are visible in two samples (C15 and C17), along with traces of carbonized plant remains.

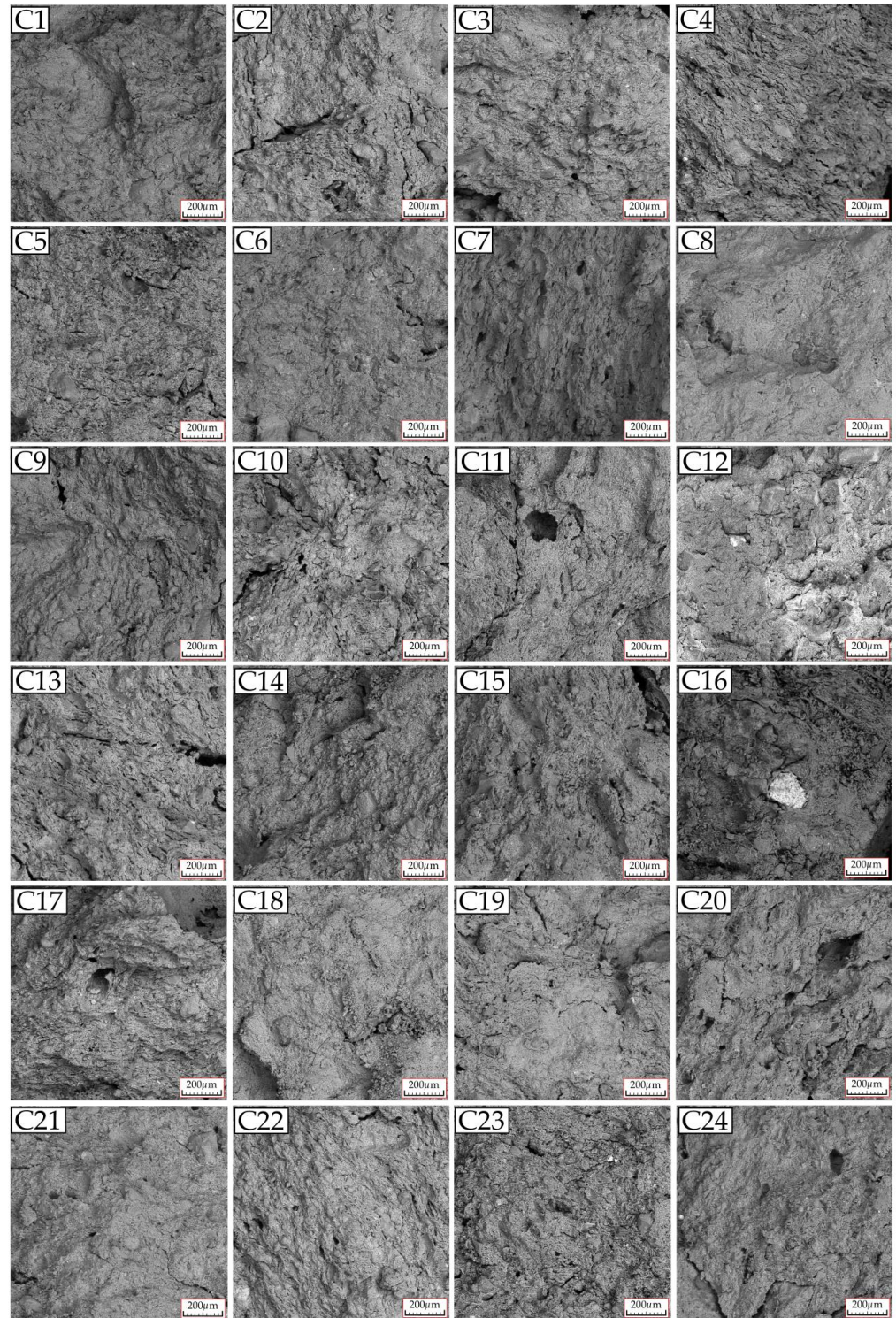
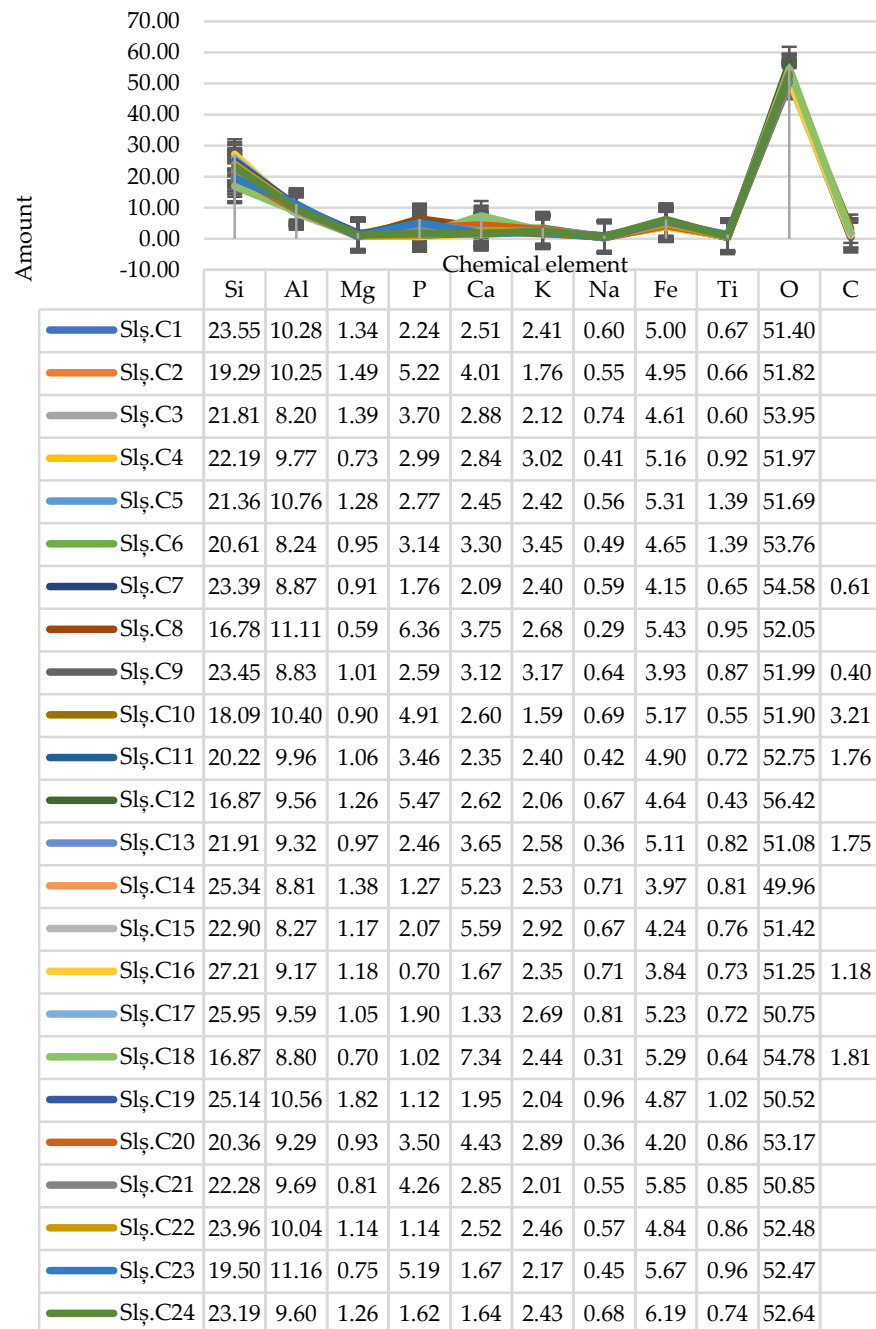


**Figure 9.** SEM micrographs of the Costișa pottery clay matrix (C1–C24) from Siliștea-Pe Cetățuie (200× magnification).

Additionally, in some samples, compact lamellar structures are visible, with elongated pores indicating the use of coil technique in vessel making (C4, C7, C13, C17, C22) [16]. However, the vitrification process was not identified in any of the samples, indicating that firing temperatures did not exceed 800–850 °C.

The EDX analysis of the Costișa matrix clay samples (Table 1) highlighted the specific elements of the raw material, such as silicon, aluminum, phosphorus, magnesium, calcium, potassium, sodium, iron, titanium, oxygen, or carbon, attributed to aluminosilicates, iron oxides, feldspars, and other mineral components present in clay [17–19].

**Table 1.** Elemental composition in weight percent (%) of the Costișa pottery clay matrix from Silișteana-Pe Cetățuie.



The elements that have archaeometric value and provide a series of data about the nature of the clay used, firing temperature, and functionality of the vessels are iron, calcium, phosphorus, and carbon [20–24].

The concentration of Fe in the analyzed samples is equal to or exceeds the threshold of 4% for all fragments, suggesting the use of ferruginous clay with high levels of iron oxides, visible in macro- and microscopic analyses [18,25,26]. Additionally, the calcium concentration surpasses the iron concentration for three fragments (C14, C15, and C18), reaching up to 7.33%. This aspect may indicate the presence of calcareous clay in their making or carbonates [25,26]. The definitive determination of the origin of the calcium concentration will also be made through  $\mu$ -FTIR analyses.

Carbon is present in the paste of seven vessels (C7, C9–C11, C13, C16, and C18), indicating a firing temperature that did not exceed 700 °C, as this element disappears from the ceramic paste at temperatures above this threshold [27–32]. The SEM analysis of these fragments, characterized by low homogeneity and individualized mineral particles, also revealed this aspect.

All fragments contained phosphorus, but 16 samples exceeded the 2% threshold, with values ranging from 2.06% to 6.36%. This high content is attributed to the fact that the fragments come from cooking or food storage vessels, like those of the *Fabaceae* family, for milk or possibly wine [33–36].

The SEM analysis performed on the core of Monteoru fragments generally showed good homogeneity, with well-integrated mineral microstructural elements in the clay mass, indicating firing at relatively high temperatures (Figure 10). The vitrification process was not identified in any sample [14,25,37]. Six samples (M5–M7, M13, M14, and M19) showed low homogeneity with well-individualized mineral components, while one sample (M16) also showed traces of carbonized plant materials.

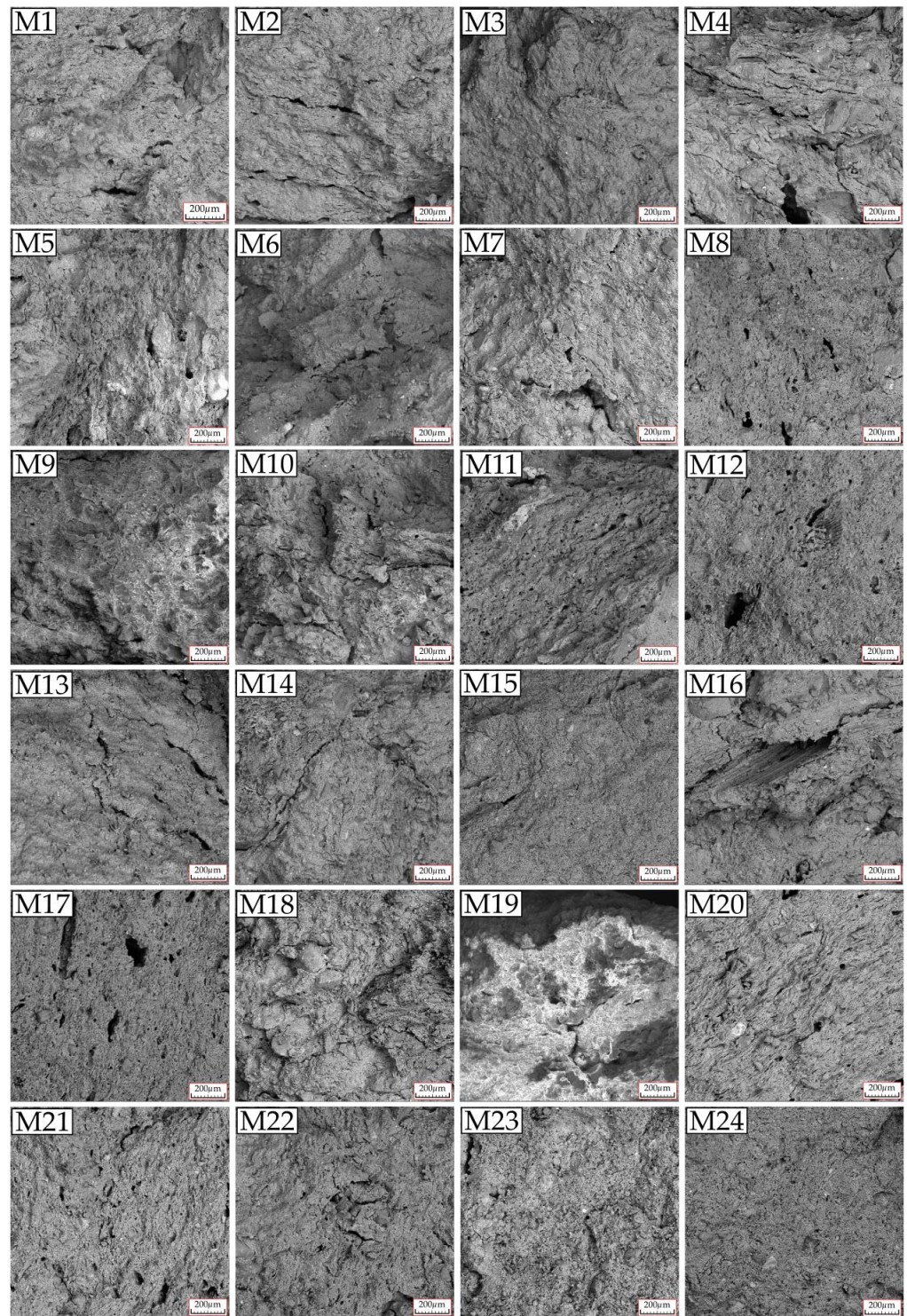
Compact lamellar structures with flattened pores, indicating the coiling technique, are visible in seven samples (M1, M2, M4, M5, M11, M20, and M21), demonstrating the microscopic use of this method in vessel making [16].

Similar to the Costișa samples, the chemical composition of the Monteoru samples contains the same specific elements derived from aluminosilicates, quartz, feldspars, mica, and iron oxides (Table 2) [17–19]. In addition to silicon, aluminum, phosphorus, magnesium, calcium, potassium, sodium, iron, titanium, oxygen, or carbon, chlorine was also identified.

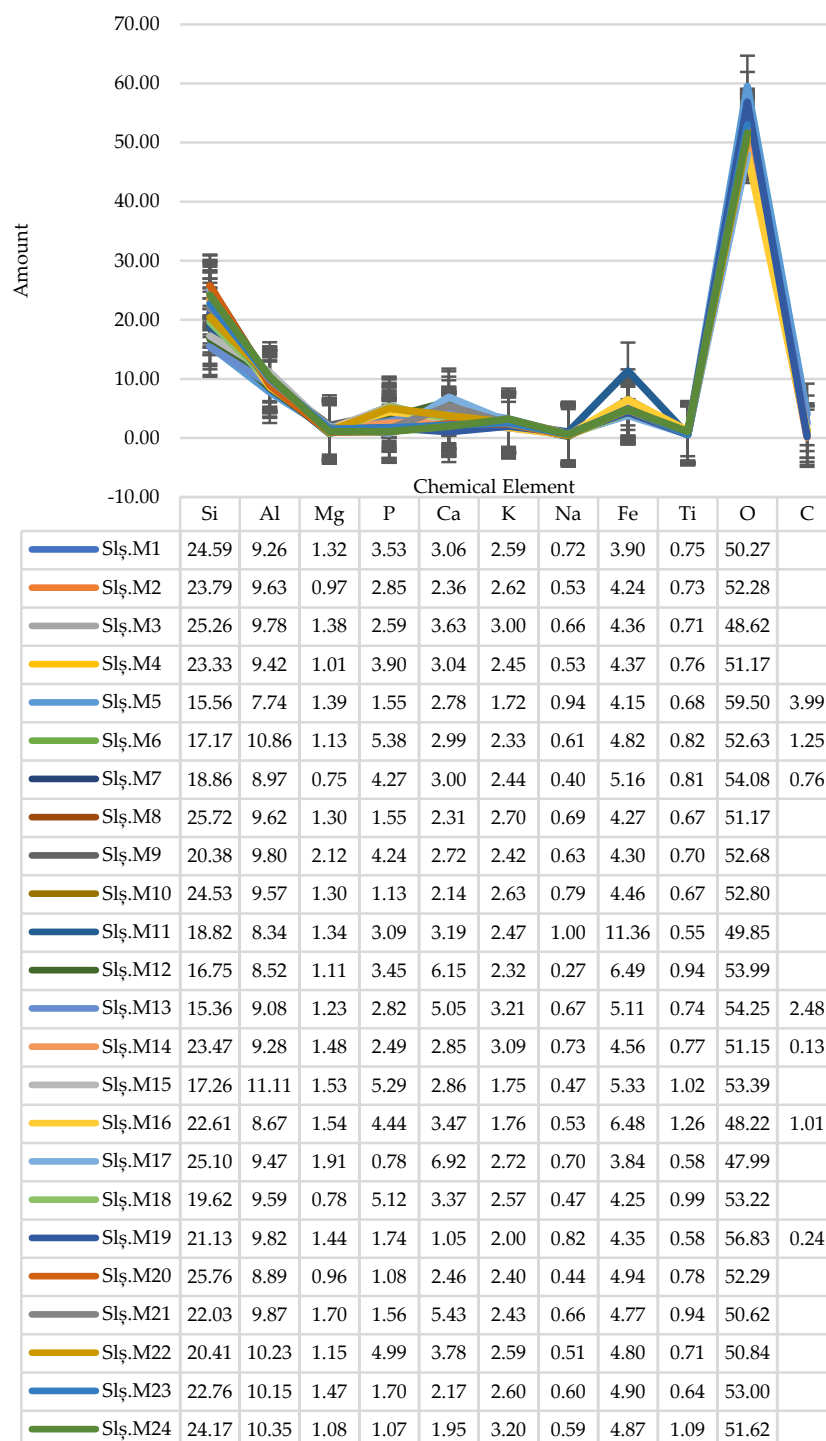
Iron is present in all analyzed samples, with concentrations ranging from 3.83% to 11.35%, indicating the use of low calcareous clay in vessel making [18,25,26]. Additionally, like the Costișa samples, four samples were identified with a high calcium content (M12, M13, M17, and M21) of up to 6.91%, which may also indicate the presence of calcareous clay or carbonates [25,27].

The presence of carbonates is noticed in seven samples (M5–M7, M13, M14, M16, M19), indicating a firing temperature below 700 °C, an aspect that will also be verified through  $\mu$ -FTIR analysis.

Phosphorus concentrations exceed 2% in 15 samples, with values ranging from 2.49% to 5.38%, suggesting that, similar to Costișa samples, they are used both in food preparation and in storing phosphorus-rich products. These concentrations may result from using the vessels for storing liquids with a high phosphorus content, such as milk or wine.



**Figure 10.** SEM micrographs of the Monteoru pottery clay matrix (M1–M24) from Siliștea-Pe Cetățuie (200× magnification).

**Table 2.** Elemental composition in weight percent (%) of the Monteoru pottery clay matrix from Silișteea-Pe Cetățuie.

### 3.1.4. $\mu$ -FTIR Analysis

The results obtained from the  $\mu$ -FTIR analysis have highlighted significant similarities regarding the chemical compounds present in the Costișa (Figure 11) and Monteoru (Figure 12) samples. Several exceptions have also been identified, which will be discussed in detail in the following sections.

In the group pottery fragments from Costișa, in the water domain, which is located between 4000 and 3000  $\text{cm}^{-1}$ , peaks attributed to hydroxyl groups (OH) are visible between 3405 and 3120  $\text{cm}^{-1}$ , and OH deformations are visible at 1513  $\text{cm}^{-1}$  and 1630  $\text{cm}^{-1}$ . These

are due to water absorbed in the ceramic samples following depositional processes or as a result of cleaning the ceramic fragments [38–44].

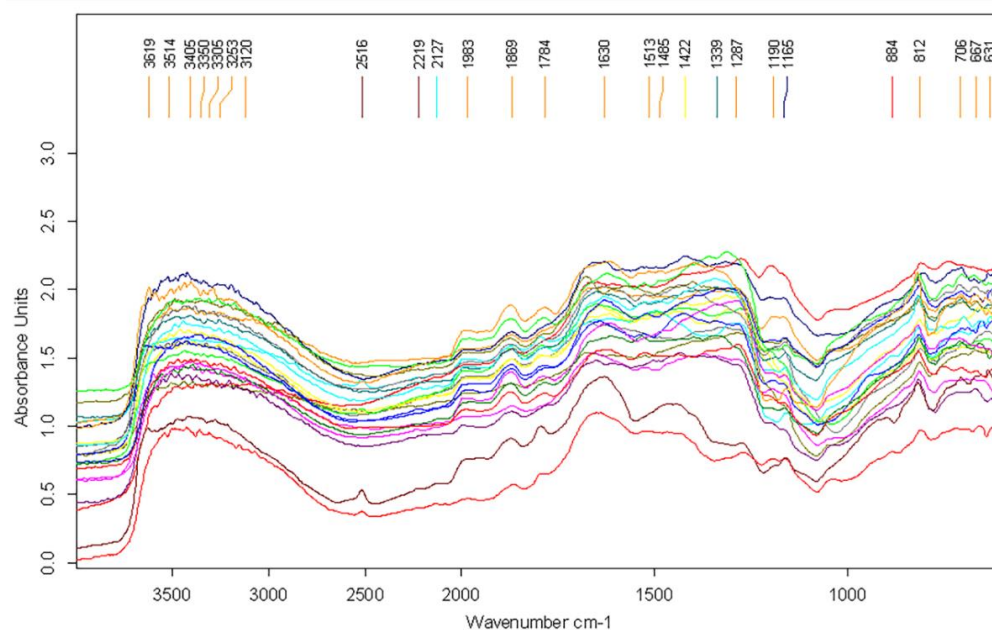


**Figure 11.** FTIR spectra for the Costișa pottery clay matrix from Siliștea-Pe Cetățuie.

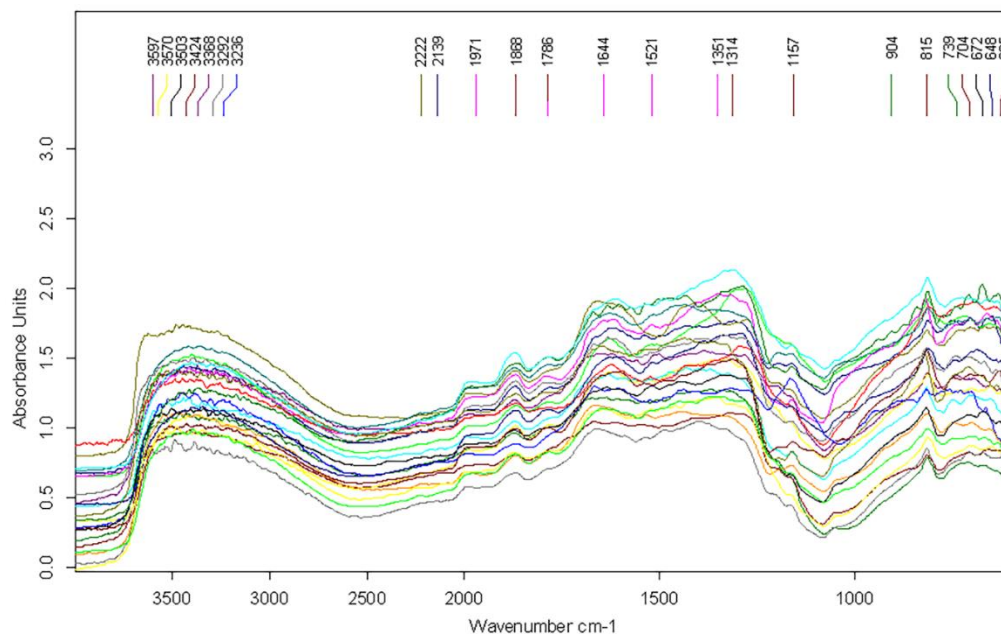


**Figure 12.** FTIR spectra for the Monteoru pottery clay matrix from Siliștea-Pe Cetățuie.

In all the analyzed samples, kaolinite ( $\text{Al}_2\text{Si}_2\text{O}_5(\text{OH})_4$ ) was identified through the peaks in the region of  $3500\text{--}3750\text{ cm}^{-1}$  [40,43,45,46]. The absence of the peak at  $\sim 3700\text{ cm}^{-1}$  and the absence of the doublets at  $915\text{ cm}^{-1}$  indicate that the vessels were fired at temperatures exceeding  $500\text{--}550\text{ }^\circ\text{C}$  [30,40,42,47–49].

Through the peaks in the range of  $1300\text{--}1500\text{ cm}^{-1}$ , the presence of carbonates was identified [29,30,50], indicating that firing temperatures did not exceed  $700\text{--}750\text{ }^\circ\text{C}$  [30,51]. This temperature range would have allowed the decomposition of calcite into gehlenite ( $\text{CaAl}_2\text{SiO}_7$ ), diopside ( $\text{CaMgSi}_2\text{O}_6$ ), and anorthite ( $\text{CaMgSi}_2\text{O}_6$ ) [28–32]. Additionally, peaks at  $2516\text{ cm}^{-1}$  and  $884\text{ cm}^{-1}$  in two samples (C3, C18) revealed the presence of



calcite [52]. Given the significant differences between these two samples and their high calcite content, it is possible that their raw materials came from different sources. The EDX analysis supports this idea in part. Aragonite was also detected at  $706\text{ cm}^{-1}$ , and it was present in almost all samples [53]. Samples C11 and C24 showed no carbonates, suggesting higher firing temperatures for these two fragments.

The silicates are well represented in the region of  $2200\text{--}1870\text{ cm}^{-1}$ , attributed to the stretching vibrations of Si-O bonds in quartz, with intense peaks at  $1983\text{ cm}^{-1}$  and  $1869\text{ cm}^{-1}$  visible in all samples [38]. Additionally, peaks at  $2219\text{ cm}^{-1}$ ,  $2127\text{ cm}^{-1}$ ,  $1167\text{ cm}^{-1}$ , and  $1165\text{ cm}^{-1}$  highlighted the presence of quartz [43,46–49,52,54]. Muscovite ( $\text{KAl}_3\text{Si}_2\text{O}_{10}(\text{OH})_2$ ), another silicate present in all samples, is visible at  $1190\text{ cm}^{-1}$  and  $812\text{ cm}^{-1}$  [32,55]. Diopside ( $\text{CaMg}[\text{Si}_2\text{O}_6]$ ) is present in all samples, with a peak at  $631\text{ cm}^{-1}$  [43,54]. These minerals represent the aluminosilicates present in the clay used for pottery manufacturing, and they were also identified through mineralogical analysis.

Other siliceous minerals identified in all samples are represented by feldspars through peaks at  $1784\text{ cm}^{-1}$  and  $1287\text{ cm}^{-1}$ , with their presence also being established through mineralogical investigations [43]. Additionally, the presence of iron oxides at  $667\text{ cm}^{-1}$  was evident in all spectra, with these originating, like the other microstructural elements, from the raw material [30,54].

The FTIR spectra for the 24 Monteoru samples show the same trend, with the same chemical compounds visible in all samples (Figure 12).

Similar to the Costișa samples, the water region, spanning from  $4000$  to  $3000\text{ cm}^{-1}$ , is well highlighted by peaks ranging from  $3424$  to  $3236\text{ cm}^{-1}$ , which serve as indicators of hydroxyl groups (OH). Additionally, OH deformations are visible at  $1521\text{ cm}^{-1}$  and  $1644\text{ cm}^{-1}$ , attributed to water absorbed in the ceramic fragments [38–44].

In all the analyzed samples, kaolinite ( $\text{Al}_2\text{Si}_2\text{O}_5(\text{OH})_4$ ) was identified through peaks in the region of  $3500\text{--}3750\text{ cm}^{-1}$ , with most of the samples being fired at temperatures above  $500\text{--}550\text{ }^\circ\text{C}$  [40,43,45,46]. In this regard, two exceptions (M3, M12) were identified where the presence of the doublet at  $904\text{ cm}^{-1}$  indicates firing at temperatures lower than  $500\text{--}550\text{ }^\circ\text{C}$  [30,45–49].

The presence of carbonates is visible in all samples through peaks in the range of  $1300\text{--}1500\text{ cm}^{-1}$ , with only one exception (M17) [29,30,50]. In all samples, aragonite is identifiable at  $704\text{ cm}^{-1}$  [53]. The presence of carbonates indicates firing temperatures below  $700\text{--}750\text{ }^\circ\text{C}$ .

Similar to the Costișa samples, the class of silicates is the most well-represented. The stretching vibrations of Si-O bonds in quartz in the region of  $2200\text{--}1870\text{ cm}^{-1}$  are highlighted by peaks at  $1971\text{ cm}^{-1}$  and  $1868\text{ cm}^{-1}$ , visible in all samples. Additionally, the presence of quartz itself was identified through peaks at  $2222\text{ cm}^{-1}$ ,  $2139\text{ cm}^{-1}$ , and  $1157\text{ cm}^{-1}$ . Other silicates found in the samples that were studied are muscovite ( $\text{KAl}_3\text{Si}_2\text{O}_{10}(\text{OH})_2$ ), which can be seen at  $815\text{ cm}^{-1}$ , and diopside ( $\text{CaMg}[\text{Si}_2\text{O}_6]$ ), which can be seen at  $625\text{ cm}^{-1}$ .

Peaks at  $1786\text{ cm}^{-1}$  confirmed the presence of feldspars, and the identification of albite ( $\text{NaAlSi}_3\text{O}_8$ ) at  $739\text{ cm}^{-1}$  and orthoclase ( $\text{KAlSi}_3\text{O}_8$ ) at  $672\text{ cm}^{-1}$  established their alkaline nature [30,43,54–56]. Iron oxides are also visible in all Monteoru fragments at  $648\text{ cm}^{-1}$ , originating, like the other minerals, from the raw material [30,54].

### 3.2. The Experiment's Results and Discussion

#### 3.2.1. Optical Microscopy and Mineralogy Analysis

Optical microscopy revealed the presence of quartz, iron oxides, feldspars, carbonates, and possibly organic matter (Figure 13). These elements are visible in all four sources of raw material, being common geological minerals in the study area.

Thus, as no major microscopic differences were observed, two sources, S2 and S4, were selected for mineralogical analysis. In this regard, considering that interdisciplinary analysis established that most of the samples were fired at temperatures ranging between  $500/550\text{ }^\circ\text{C}$  and  $700/750\text{ }^\circ\text{C}$ , the samples chosen for mineralogical analysis were those fired at  $700\text{ }^\circ\text{C}$ .

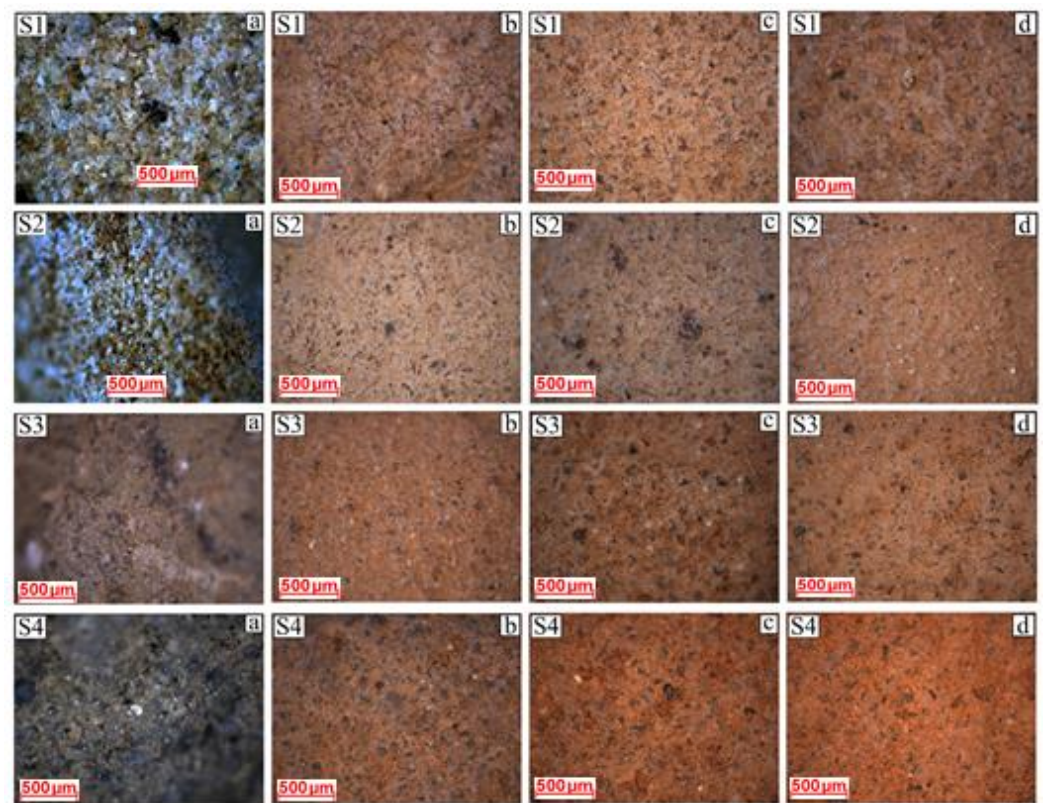


**Figure 13.** OM images of the clay samples used in the experimental study: (a) unfired clay; (b) 450 °C; (c) 700 °C; (d) 900 °C (50× magnifications).

Thus, source S2, originating from the clay deposit located 250 m from the settlement, was mineralogically more complex (Figure 14). This sample contains granules of monoclinic quartz (angular and subangular), muscovite, plagioclase feldspars, sandstone lithoclaste, oolites, and calcite. The identification of calcite is explained by the fact that the decomposition temperature of 750 °C was not reached, which supports and reinforces the results of the chemical analyses. Additionally, bioclasts such as foraminifera of the *Ammonia beccarii* type, *Porosonion subranosus*, *Bulimina* sp., and remnants of calcareous algae were identified in this sample. These are specific to Sarmatian deposits, indicating calcareous clay.

In sample S4 (Figure 15), sub-angular and sub-rounded grains of mono- and polycrystalline quartz, muscovite, hematitic aggregates, and plagioclase feldspars were identified. The presence of polycrystalline quartz crystal clasts, determined by the firing temperature, is of particular importance, as they show clear similarities with the ceramic fragments from Costișa and Monteoru. Additionally, the presence of a lithoclast derived from volcanic rock, resulting from the deposition of sediments transported by the Bistrița River from the mountainous area, is noteworthy as it is a common occurrence in the geology of the Siliștea-Pe Cetățuie settlement area. Furthermore, in addition to these mineral elements, a bioclast represented by a plant fragment was also identified.

The microscopic observations conducted highlighted the presence of common clay elements such as quartz, mica, carbonates, and organic matter. The mineralogical results complemented these findings by identifying feldspars, various lithoclasts (sandstones, volcanic rock fragments), and plant remains.

From a mineralogical perspective, source S4 represents the possible source of clay used in pottery manufacturing. The presence of polycrystalline quartz, which demonstrated the same type of modifications as those observed after firing, supports this statement, indicating the same quartz-rich clay as in the ceramic vessels. Bioclasts like foraminifera and elements like oolites were only found in source S2, which supports this conclusion even more, not being found in the clay that was used to manufacture the ceramic vessels.

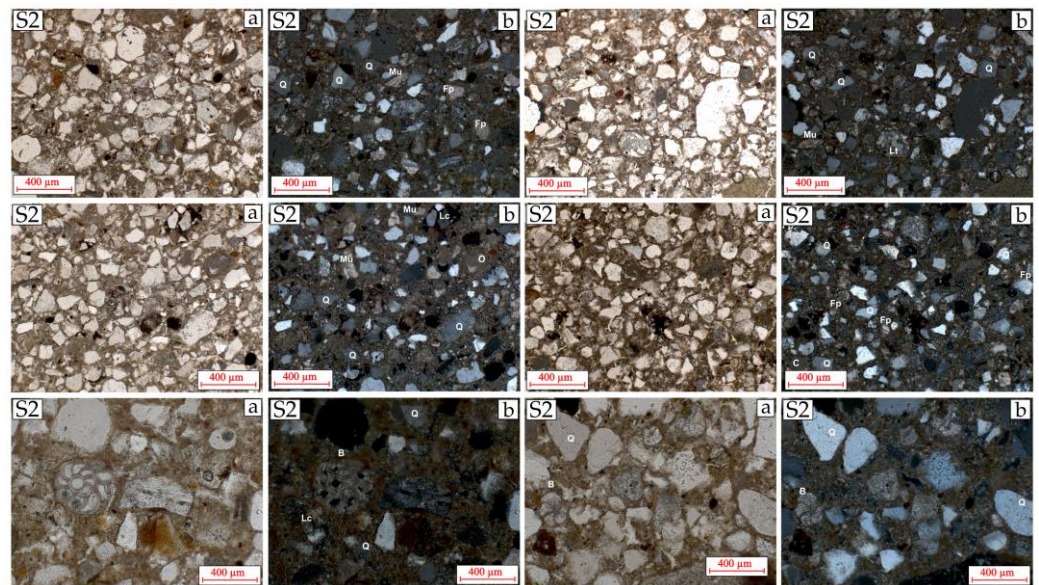


**Figure 14.** Mineralogical section of sample S2: Q—quartz; Lc—limestone lithoclaste; Mu—muscovite; Fp—plagioclase feldspars; C—calcite; O—oolite; B—foraminifera *Ammonia beccarii*, *Porosonion subranosus*, and *Bulimina* sp. and calcareous algae ((a): parallel nicoli; (b): crossed nicoli).

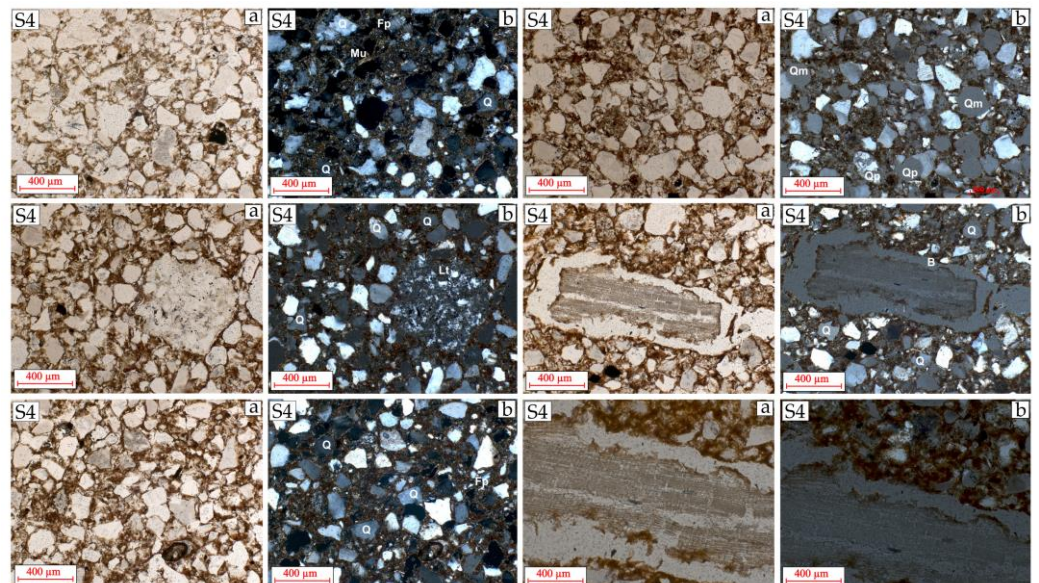


**Figure 15.** Mineralogical sections of sample S4: Q—quartz; Qm—monocrystalline quartz; Qp—polycrystalline quartz; Lt—possible volcanic lithoclast; Mu—muscovite; Fp—plagioclase feldspars; C—calcite; B—plant fragment ((a): parallel nicoli; (b): crossed nicoli).

### 3.2.2. EDX Analysis

EDX analyses were performed for all four clay sources, both for the raw clays and for the three firing stages. The results show that sources S1, S2, and S3 are calcareous clays [25,27], with calcium levels reaching 10–11% (Table 3 (S1, S2 and S3)). Source S4, on the other hand, has calcium levels lower than 1% and iron levels higher than 4%, which means it is a ferruginous clay [17,26] (Table 3 (S4)). In this regard, the iron concentration exceeds 4% only in sample S4, which is similar to those found in the ceramic fragments.

**Table 3.** Elemental compositions of the clay sources: S1, S2, S3, and S4.

	Si	Al	Mg	P	Ca	K	Na	Fe	Ti	O	C
<i>S1 unburned</i>	29.81	4.04	1.20	0.16	4.84	2.19	0.77	2.27	0.31	53.09	1.31
<i>S1 450 °C</i>	21.46	5.71	1.66	0.07	10.58	3.26	0.36	3.83	0.71	51.75	0.61
<i>S1 700 °C</i>	26.18	5.65	1.75	0.19	8.26	2.51	0.47	3.03	0.41	51.55	0.00
<i>S1 900 °C</i>	25.88	5.98	1.82	0.24	9.31	2.55	0.45	3.36	0.47	49.93	0.00
	Si	Al	Mg	P	Ca	K	Na	Fe	Ti	O	C
<i>S2 unburned</i>	14.78	5.61	2.26	0.15	14.78	3.55	0.48	2.44	0.49	52.23	3.23
<i>S2 450 °C</i>	23.76	6.85	2.18	0.24	8.77	2.58	0.38	3.65	0.53	50.46	0.60
<i>S2 700 °C</i>	24.36	6.72	2.08	0.18	9.08	2.70	0.52	3.43	0.56	50.36	0.00
<i>S2 900 °C</i>	24.02	6.67	2.30	0.19	11.28	2.98	0.47	3.70	0.69	47.71	0.00
	Si	Al	Mg	P	Ca	K	Na	Fe	Ti	O	C
<i>S3 unburned</i>	20.71	6.49	1.72	0.64	9.40	2.24	0.83	2.58	0.49	54.42	0.48
<i>S3 450 °C</i>	27.48	5.98	1.14	0.27	7.14	2.30	0.37	3.42	0.45	51.21	0.25
<i>S3 700 °C</i>	26.70	6.29	1.28	0.26	6.95	2.28	0.60	3.58	0.53	51.27	0.27
<i>S3 900 °C</i>	25.76	6.56	1.31	0.22	8.64	2.36	0.51	3.69	0.43	50.52	0.00
	Si	Al	Mg	P	Ca	K	Na	Fe	Ti	O	C
<i>S4 unburned</i>	25.12	7.03	1.30	0.19	0.99	2.49	0.58	4.22	0.76	54.49	2.83
<i>S4 450 °C</i>	30.16	7.54	1.26	0.23	0.84	2.14	0.75	3.97	0.65	52.27	0.19
<i>S4 700 °C</i>	31.06	7.14	1.27	0.28	0.96	2.10	0.49	4.07	0.80	51.71	0.10
<i>S4 900 °C</i>	32.66	7.08	1.21	0.22	0.73	1.69	0.53	4.24	0.40	51.25	0.00

Therefore, a comparison between the elemental compositions of the clay sources and the Costișa and Monteoru ceramic fragments revealed similarities with source S4. These findings support the mineralogical observations, which indicated the use of the same source in vessel manufacturing. As noted in the interdisciplinary analyses conducted on the ceramic fragments, the exceptions represented by the two Costișa samples (C3 and C18) suggest the use of another source, most likely S2, as their compositions are very similar. This information will be verified through  $\mu$ -FTIR analyses.

Furthermore, the differences in phosphorus concentrations between the clay sources and the ceramic fragments, which do not exceed 1% in the test samples, can be clearly observed. This observation, along with data obtained from soil samples, supports and reinforces the origin of this element from the use of vessels for cooking or storing goods or liquids rich in phosphorus.

### 3.2.3. $\mu$ -FTIR Analysis

Infrared spectroscopy was conducted for all four clay sources at all firing stages (Figure 16) to observe the chemical changes occurring in the clay at specific temperatures and to understand how these reactions alter the overall appearance of the spectra.

The water region, located between 4000 and 3000  $\text{cm}^{-1}$ , is very intense at 450 °C, then gradually decreases until 900 °C as the chemically bound water is eliminated [38,39]. Additionally, the OH deformations visible at 1634  $\text{cm}^{-1}$  exhibit the same decreasing behavior, which is directly proportional to the temperature values [40–44].

The kaolinitic clay represents the four sources with peaks in the 3500–3750  $\text{cm}^{-1}$  region [40,43,45,46]. In the case of kaolinite, a decrease in intensity is also observed, and at 450 °C, the doublet at 924  $\text{cm}^{-1}$  is visible, indicating that the firing temperature did not exceed 500–550 °C [30,40,42,47]. At the firing temperature of 700 °C, this doublet disappears, and at 900 °C, it is only detectable in one sample, indicating the formation of amorphous silica of metakaolinite [57]. The increase in the intensity of the silicate region at approximately 2200–1800  $\text{cm}^{-1}$  supports this aspect [38,58].

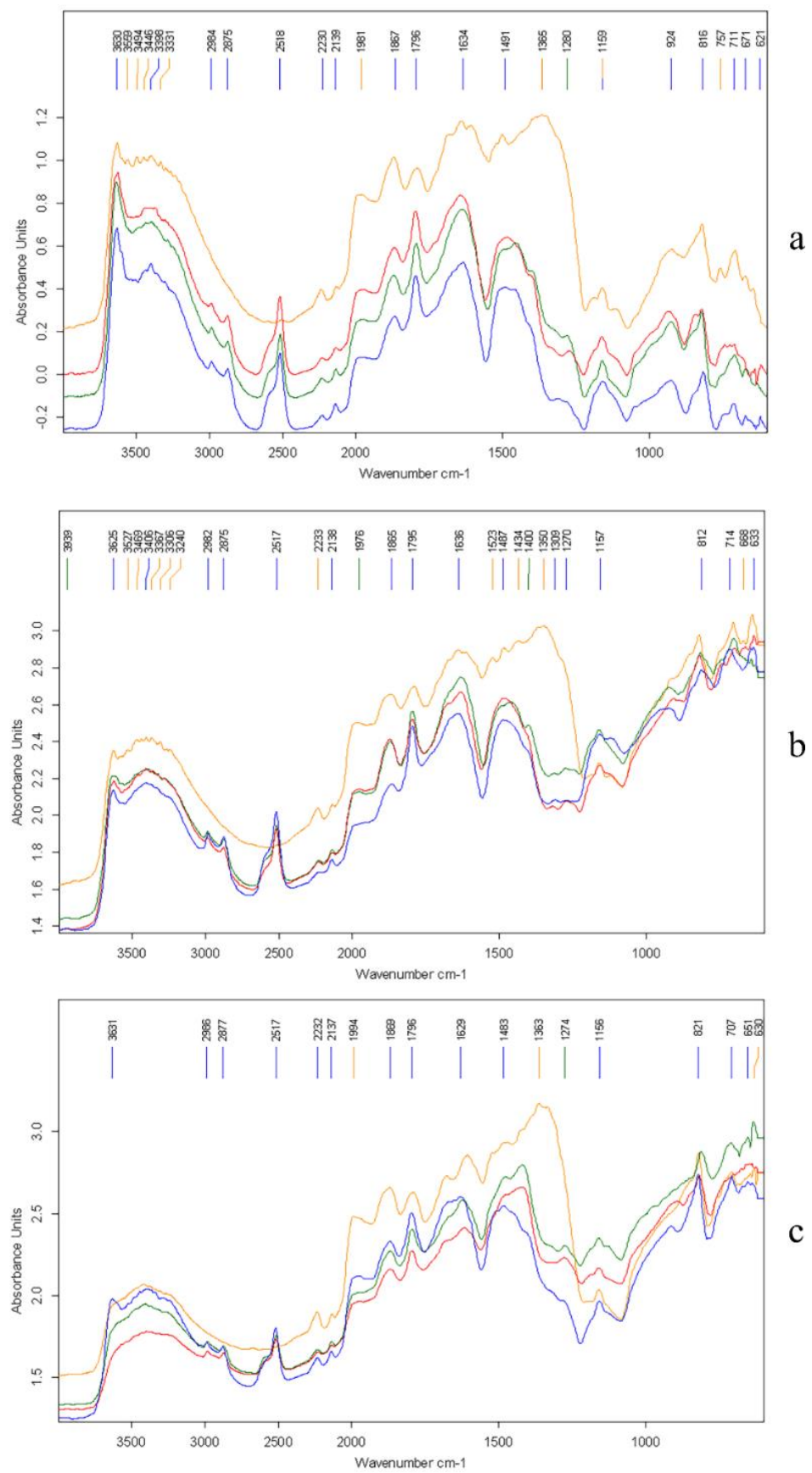


**Figure 16.** FTIR spectra for the clay sources: (a)—450 °C; (b)—700 °C; (c)—900 °C (Blue—S1; Red—S2; Green—S3; Orange—S4).

The range of 1300–1500  $\text{cm}^{-1}$  is specific to carbonates until the temperatures of 700–750  $^{\circ}\text{C}$  exhibit a broad band in the specific interval. At 900  $^{\circ}\text{C}$ , this band narrows, showing the peak at 1363  $\text{cm}^{-1}$  for S4 and the one at 1483  $\text{cm}^{-1}$  for S1, S2, and S3 [28,30,50,51]. Furthermore, sources S1, S2, and S3 contain visible calcite through peaks at 2984  $\text{cm}^{-1}$ , 2875  $\text{cm}^{-1}$ , 2518  $\text{cm}^{-1}$ , and 711  $\text{cm}^{-1}$  [52]. The intensity of these peaks decreases toward 900  $^{\circ}\text{C}$  due to their decomposition. EDX analyses support this aspect, demonstrating the decomposition of  $\text{CaCO}_3$  and the formation of  $\text{CaO}$  through the disappearance of carbon.

The silicates are well represented in the region of 2200–1870  $\text{cm}^{-1}$ , attributed to the stretching vibrations of Si-O bonds in quartz. Peaks at 1280  $\text{cm}^{-1}$ , 1159  $\text{cm}^{-1}$ , 757  $\text{cm}^{-1}$ , 707  $\text{cm}^{-1}$ , and 668  $\text{cm}^{-1}$  also indicate the presence of quartz. Another silicate identified in all samples is muscovite, which is visible at 816  $\text{cm}^{-1}$ . These minerals constitute aluminosilicates present in the clay sources, and they were identified through mineralogical analysis as well. Mineralogical investigations confirmed the presence of feldspars and other siliceous minerals identified in all samples, as indicated by the peak at 1776  $\text{cm}^{-1}$ .

Additionally, the presence of iron oxides was observed in all spectra. At 450  $^{\circ}\text{C}$ , these appear as magnetite, indicated by the peak at 671  $\text{cm}^{-1}$ , which transforms into hematite at temperatures higher than 600  $^{\circ}\text{C}$ , visible at 633  $\text{cm}^{-1}$  and 630  $\text{cm}^{-1}$ .

The  $\mu$ -FTIR analysis illustrates the differences between the four raw material sources, highlighting the calcareous nature of sources S1, S2, and S3, while source S4 indicates a ferruginous clay. Additionally, this analysis has highlighted the chemical changes described in the existing literature, confirming the interpretations of the results obtained for the ceramic fragments.

By comparing the FTIR spectra of the clay sources (S1–S4) with those of the ceramic fragments (Costișa and Monteoru), it was indicated that the raw material source used in pottery manufacturing was source S4.

#### 3.2.4. Thermal Analysis

A set of thermal tests were conducted on four samples, two Costișa (C3, C24) and two Monteoru (M17, M21), to confirm the firing temperatures found through chemical tests. These samples were selected because two of them (C3, M21) contain carbonates, while the other two do not (C24, M17). Thus, TGA and DTA analyses will contribute to strengthening the conclusions drawn from the analytical techniques applied to the pottery samples. Additionally, one sample from source S2 and one from source S4 were also analyzed, serving as a comparative element for studying the chemical changes occurring in the raw material during firing.

The samples were fired in the thermobalance furnace up to 1000  $^{\circ}\text{C}$  in an air atmosphere. The variation in mass was measured and represented graphically (expressed as a percentage of the initial sample mass) as a function of the sample temperature—TG curves. The derivatives of the TG curves (DTG curves) better highlight the temperature ranges where mass variation processes occur. The thermal effects, with heat absorption (endothermic) or release (exothermic)—DTA curves, were also illustrated.

The clay sample from source S2 is thermally unstable; initially, it showed a large mass loss of approximately 6%, likely due to the burning of organic matter residues or moisture. Subsequently, it continues to lose mass continuously, starting at 400  $^{\circ}\text{C}$ , with a visible endothermic effect at 450–650  $^{\circ}\text{C}$  in the DTA curve. The calcination of calcium carbonate causes a distinct, endothermic stage of rapid mass loss, approximately 7%, in the temperature range of 700–850  $^{\circ}\text{C}$ . The mass of the clay sample from source S2 continues to decrease to approximately 84% upon heating to 1000  $^{\circ}\text{C}$  (Figure 17).

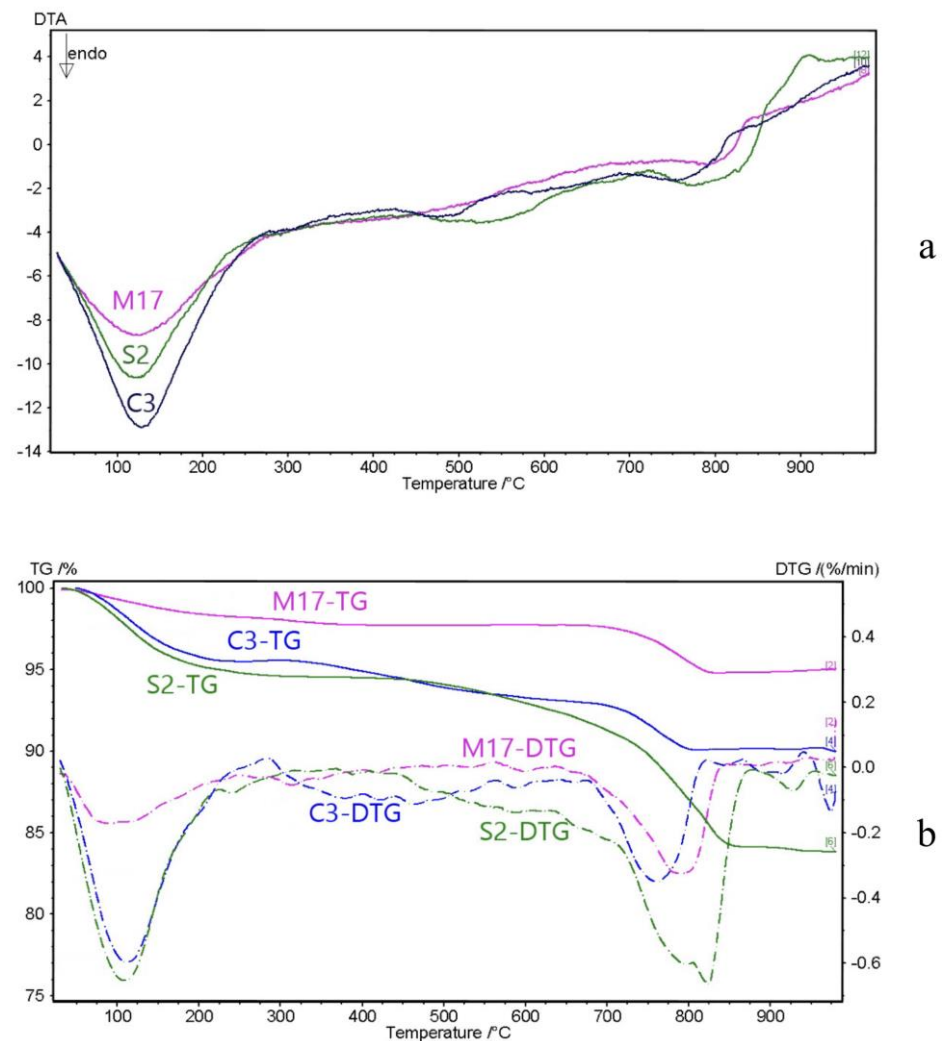


**Figure 17.** DTA (a) and TG/DTG (b) curves for samples C3, M17, and source S2.

Sample M17 shows a mass loss of up to 300 °C due to the evaporation of absorbed water, which is very small, approximately 2%. The mass then remains constant until ~700 °C, indicating an initial firing that reached this temperature. The higher porosity of the ceramic fragment caused a mass loss of approximately 4.5% in Sample C3 due to water evaporation. A slight mass increase is observed around 300 °C, indicating oxidation processes without the formation of volatile products. A slow mass loss occurs between 400 and 700 °C, followed by an endothermic effect in the DTA curve between 400 and 550 °C (Figure 18). This indicates a lower stabilization of sample C3 compared to sample M17, probably caused by the initial firing at lower temperatures. Between 700 and 850 °C, both ceramic samples lose about 3% of their mass. The DTA curve also shows an endothermic effect, which is the same as what happened with the clay sample from source S4. Therefore, it is plausible that both sample M17 and sample C3 originate from the clay from source S4, but sample M17's superior initial firing resulted in greater stability up to 700 °C compared to sample C3. The mass stability between 850 and 1000 °C for the ceramic samples compared to source S4 indicates a clear consolidation of the ceramic fragments following the initial firing. Additionally, the initial firing resulted in a smaller mass loss at 800 °C and a shorter time interval for the ceramic samples compared to the clay sample from source S4.

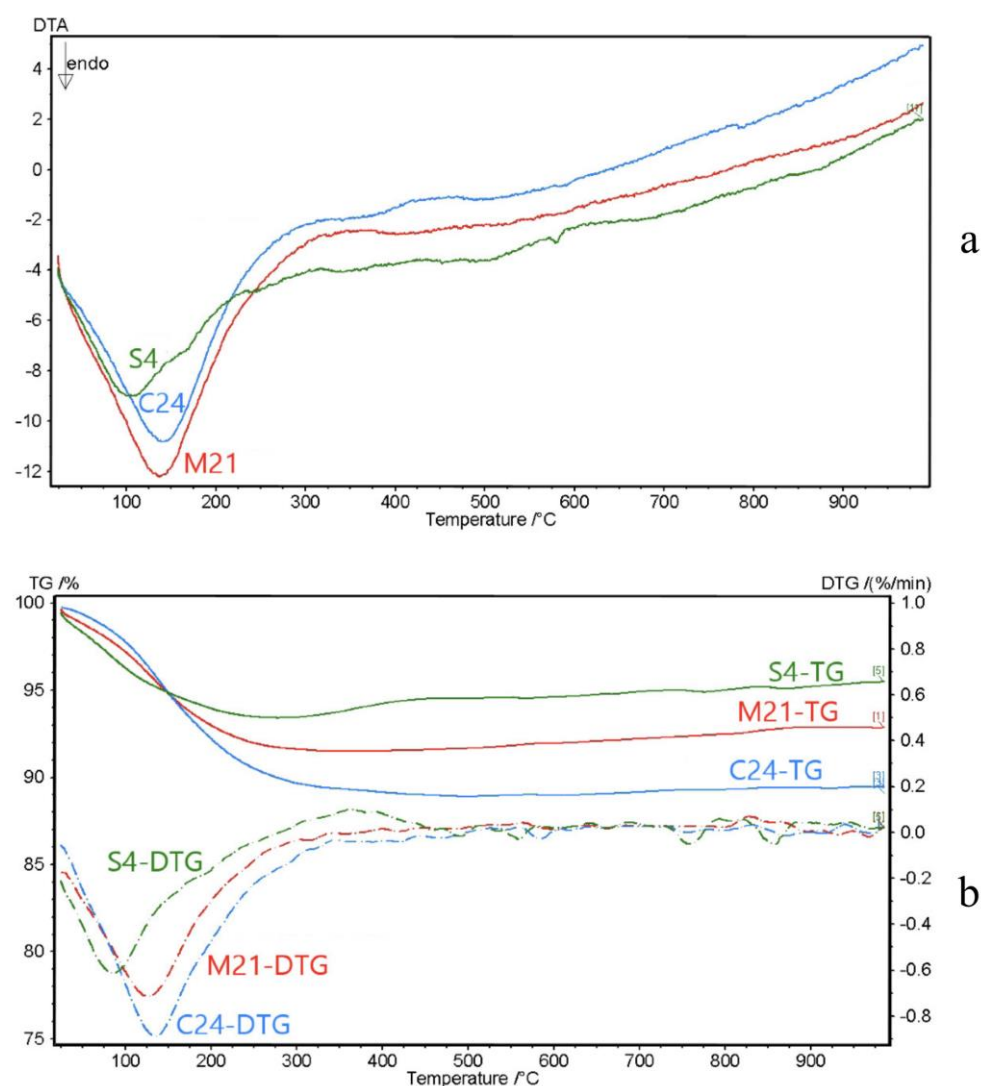


**Figure 18.** DTA (a) and TG/DTG (b) curves for samples C24, M21, and source S4.

The clay sample from source S4 is much more thermally stable than that from source S2. After burning off impurities with a mass loss of approximately 7% up to 300 °C, the sample shows a mass increase in the 300–500 °C interval due to stabilization processes by firing, with the increase continuing slowly up to 1000 °C. Sample M21 also shows a continuous mass increase above 300 °C, but this is less pronounced than in the case of the clay sample from source S4, indicating stabilization following the initial firing. In contrast, sample C24 exhibits no mass variations or thermal effects above 300 °C, suggesting a strong stabilization of its composition and structure, likely due to an initial firing process at high temperatures.

The results obtained from this type of analysis illustrate firing temperatures between 550 and 700 °C, confirming the information obtained through SEM-EDX and  $\mu$ -FTIR techniques. These results support the hypothesis of firing in pits or above ground, with different temperatures resulting from relatively low control of pyrotechnological installations, leading to a wide range of colors. Additionally, similarities in TG, DTG, and DTA curves were observed through this method, indicating that the ceramic fragments from Costișa and Monteoru were made from clay sourced from S4.

Regarding the pyrotechnological elements, interdisciplinary studies have established that the Costișa and Monteoru pottery from Siliștea-Pe Cetățuie was fired at temperatures ranging between 500/550 °C and 700/750 °C. The fact that these temperatures do not



correspond to certain types of vessels, the firing atmosphere is not uniform, and the colors of the vessels are relatively different suggests that the vessels of both communities were fired in pits or above ground.

#### 4. Conclusions

The archaeometric analysis of the ceramic assemblages from the Silișteea-Pe Cetățuie settlement has established both general and specific aspects of the pottery of these two communities. Both ceramic groups used the same technique to make their vessels, primarily using local ferruginous clay from the settlement's immediate vicinity and a calcareous clay from approximately 250 m. The precise identification of the source of the raw material has highlighted the behavior of the Costișa and Monteoru communities regarding the resource catchment area, with a preference for the proximity of the settlement, which facilitates rapid access with minimal effort. Additionally, both pottery groups used ceramoclasts in their paste, identifying three distinct categories for specific functional classes in both Costișa and Monteoru vessels. Moreover, in the case of both communities, reused ceramic clasts were identified, which could have a dual role, one of a practical and technological nature and the other a distinct socio-cultural role.

Through the proposed experiment and the methodology used, the source of the raw material used by the potters of the Costișa and Monteoru ceramic groups from the settlement of Silișteea-Pe Cetățuie has been identified. The mineralogical, chemical, and thermal analyses have demonstrated that the raw material was extracted from the immediate vicinity of the settlement plateau, approximately 60 m from the inhabited area.

An ecological perspective can explain this aspect as individuals adapt to their surrounding environment. Despite its apparent use, the presence of only two clay fragments does not suggest a preference for the source located approximately 250 m away. The potters opted for an immediate and easily accessible source. The production of pottery requires a considerable amount of raw material, involving a significant effort in procurement and, especially, transportation. Therefore, the preference for using clay located near the settlement is easily understood. In this regard, the positioning of the settlement was determined by several factors. Besides its defensive nature, it provided the necessary conditions for subsistence. Thus, the resource catchment area can be estimated at approximately 600 m from the settlement, within which water and clay sources were found. Therefore, Bronze Age communities chose the simplest route to obtain the necessary reserves. Furthermore, whether the potters were aware of it or not, the functional characteristic, which uses quartzose clay to enhance the quality of the vessels, complements this environmental adaptability. However, the functional component appears to have played a marginal role in selecting the raw material source. In this sense, the central and constant elements of pottery manufacturing for both communities are represented by the use of ceramoclasts, which, besides their technological benefits, most likely represent an assumed socio-cultural behavior. This aspect can be correlated in a more extensive space and to the southern area of Romania, where the study that had the same subject shows a cultural tradition linked to the use of certain sources since the Eneolithic period [4].

Following the presentation of the investigations conducted for the Silișteea-Pe Cetățuie settlement, a series of important observations regarding Middle Bronze Age pottery were made. These observations provide significant contributions to establishing prehistoric behavioral patterns regarding the exploitation of clay sources used in this activity. Starting from the premise of using sources as close as possible to the inhabited area, samples were taken from the proximity of the settlements, a hypothesis confirmed in the case of the Silișteea site. This aspect was explained by a series of geographical factors related to the difficulty of accessibility of the settlement, such as the steep slope (between 26.5–45.1%), the degree of anthropic fortification (a defense ditch about 3 m deep), and the altitude (448 m), as well as factors such as proximity to the water source (approximately 600 m). In this case, the effort of procuring raw materials seems unjustified in terms of the large amount of energy required for this stage of the technological chain. However, the identification of

pottery fragments made from clay located at a greater distance could indicate, in the case of the Costișa community, the influence of cultural or religious elements.

The information about how clay sources were used at different times in prehistory shows the need to look at more sites from both a synchronic and a diachronic point of view to get a fuller and more accurate picture of how resources were selected and used, as well as the behaviors of people that led to the exploitation of the environment.

**Author Contributions:** Conceptualization, A.D. and N.B.; methodology, A.D. and V.V.; software, A.D., V.V., N.B., B.-G.R. and M.B.; validation, A.D., V.V. and N.B.; formal analysis, A.D., V.V., N.B., B.-G.R. and M.B.; investigation, A.D., V.V., N.B., B.-G.R. and M.B.; resources, A.D., V.V., N.B., B.-G.R. and M.B.; data curation, A.D., V.V. and N.B.; writing—original draft preparation, A.D.; writing—review and editing, A.D., V.V., N.B., B.-G.R. and M.B.; visualization, A.D., V.V. and N.B.; supervision, A.D., V.V. and N.B.; project administration, A.D.; funding acquisition, V.V. All authors have read and agreed to the published version of the manuscript.

**Funding:** This work was supported by a grant from the “Alexandru Ioan Cuza” University of Iasi, within the Research Grants program, Grant UAIC, code GI-UAIC-2023-03.

**Data Availability Statement:** Data are contained within the article.

**Conflicts of Interest:** The authors declare no conflicts of interest.

## References

- Gliozzo, E. Ceramics investigation: Research questions and sampling criteria. *Archaeol. Anthropol. Sci.* **2020**, *12*, 202. [CrossRef]
- Montana, G. Ceramic raw materials: How to recognize them and locate the supply basins—Mineralogy, petrography. *Archaeol. Anthropol. Sci.* **2020**, *12*, 175. [CrossRef]
- Drob, A. Analiza Interdisciplinară a Olăriei Bronzului Mijlociu din Bazinul Bistriței. Ph.D. Thesis, Alexandru Ioan Cuza University, Iași, Romania, 2024.
- Koutouvaki, E.; Amicone, S.; Kristew, A.; Ștefan, C.E.; Berthold, C. Shared traditions and shard conservatism: Pottery making at the Chalcolithic site of Radovanu (Romania). *Archaeol. Anthropol. Sci.* **2021**, *13*, 206. [CrossRef]
- Gualtieri, S. Ceramic raw materials: How to establish the technological suitability of a raw material. *Archaeol. Anthropol. Sci.* **2020**, *12*, 183. [CrossRef]
- Hein, A.; Kilikoglou, V. Ceramic raw materials: How to recognize them and locate the supply basins: Chemistry. *Archaeol. Anthropol. Sci.* **2020**, *12*, 180. [CrossRef]
- Ménager, M.; Esquivel, P.F.; Conejo, P.S. The use of FT-IR spectroscopy and SEM/EDS characterization of slips and pigments to determine the provenances of archaeological ceramics: The case of Guanacaste ceramics (Costa Rica). *Microchem. J.* **2021**, *162*, 105838. [CrossRef]
- Bolohan, N.; Munteanu, R.; Dumitroaia, G. Siliștea, com. Români, jud. Neamț, CCA (Campania 2000), 2001, București, 229. Available online: <https://cronica.cimec.ro/detaliu.asp?k=1127> (accessed on 1 June 2024).
- Bolohan, N. “All in one”. Issues of Methodology, Paradigms and radiocarbon Datings Concerning the Outer Eastern Carpathian Area. In *Signa Praehistorica. Studia in Honorem Magistri Attila László Septuagesimo Anno. Honoraria*, 9th ed.; Bolohan, N., Mățău, F., Tencariu, A.-F., Eds.; Alexandru Ioan Cuza University: Iași, Romania, 2010; pp. 229–244.
- Bolohan, N. Settlement system during Middle Bronze Age in the south-western area of the Cracău-Bistrița basin, eastern Romania. In *Prehistoric Settlements: Social, Economic and Cultural Aspects. Seven Studies in the Carpathian Area*; Gogâltan, F., Cordoș, C., Eds.; Editura Mega: Cluj-Napoca, Romania, 2016; pp. 73–86.
- Bolohan, N.; Gafincu, A. Raport de cercetare arheologică sistematică. Șantierul arheologic Siliștea-Pe Cetățuie, jud. Ne-amț. Campania 5–19 iulie 2018, Manuscris.
- Bolohan, N.; Gafincu, A.; Drob, A. Raport de Cercetare Arheologică Sistematică. Șantierul Arheologic Siliștea-Pe Cetățuie, jud. Neamț. Campania 13–27 Iulie 2019, Manuscris. Available online: <https://cronica.cimec.ro/detaliu.asp?k=6430&d=Silistea-Romani-Neamt-Pe-Cetatuie-2019> (accessed on 1 June 2024).
- Bong, W.S.K.; Matsumura, K.; Nakai, I. Firing Technologies and Raw Materials of Typical Early and Middle Bronze Age Pottery from Kaman-Kalehöyük: A Statistical and Chemical Analysis. *Archaeol. Anthropol. Sci.* **2008**, *XVII*, 295–311.
- Amicone, S.; Radivojević, M.; Quinn, P.S.; Berthold, C.; Rehren, T. Pyrotechnological connections? Re-investigating the link between pottery firing technology and the origins of metallurgy in the Vinča Culture, Serbia. *J. Archaeol. Sci.* **2020**, *118*, 105123. [CrossRef]
- Maniatis, Y.; Simopoulos, A.; Kostakis, A.; Perdikatsis, V. Effect of reducing atmosphere on minerals and iron oxides developed in fired clays: The role of Ca. *J. Am. Ceram. Soc.* **1983**, *66*, 773–781. [CrossRef]
- Palanivel, R.; Meyvel, S. Microstructural and microanalytical study—(SEM) of archaeological pottery artifacts. *Rom. J. Phys.* **2010**, *55*, 333–341.

17. Vasilache, V.; Sandu, I.; Enea, S.C.; Sandu, I.G. Determinări ceramografice pe loturi din siturile Costești și Giurgești. In *Comunitățile Cucuteniene din Zona Târgului Frumos: Cercetări Interdisciplinare în Siturile de la Costești și Giurgești*; Boghian, D., Enea, S.C., Ignătescu, S., Stanc, S.M., Eds.; Alexandru Ioan Cuza University: Iași, Romania, 2014; pp. 138–147.
18. Sandu, I.; Vasilache, V.; Tencariu, F.-A.; Cotiugă, V. *Conservarea Științifică a Artefactelor din Ceramic*; Alexandru Ioan Cuza University: Iași, Romania, 2010.
19. Sandu, I.; Cotiugă, V.; Sandu, A.V.; Ciocan, A.C.; Olteanu, G.I.; Vasilache, V. New archaeometric characteristics for ancient pottery identification. *Int. J. Conserv. Sci.* **2010**, *1*, 75–82.
20. Bakkevig, S. Phosphate analysis in archaeology-problems and recent progress. *Nor. Archaeol. Rev.* **1980**, *13*, 73–100. [[CrossRef](#)]
21. Keeley, H.C.M. Recent work using soil phosphorus analysis in archaeological prospection. *ArchéoSci. Rev. D'Archéométrie* **1981**, *5*, 89–95. [[CrossRef](#)]
22. Kshirsagar, A. Soil Phosphorus Distribution Within Human Activity Areas at Kuntasi. *Bull. Deccan Coll. Res. Inst.* **1991**, *51–52*, 497–500.
23. Golyeva, A.; Khokhlova, O.; Lebedeva, M.; Shcherbakov, N.; Shuteleva, I. Micromorphological and Chemical Features of Soils as Evidence of Bronze Age Ancient Anthropogenic Impact (Late Bronze Age Muradymovo Settlement, Ural Region, Russia). *Geosciences* **2018**, *3*, 313. [[CrossRef](#)]
24. Salisbury, R.B. Advances in Archaeological Soil Chemistry in Central Europe. *Interdiscip. Archaeol. Nat. Sci. Archaeol.* **2020**, *XI*, 199–211. [[CrossRef](#)]
25. Maniatis, Y.; Tite, M.S. Technological Examination of Neolithic-Bronze Age Pottery from Central and Southeast Europe and from the Near East. *J. Archaeol. Sci.* **1981**, *8*, 59–76. [[CrossRef](#)]
26. Nadeau, P.H.; Tite, J.M. Transmission electron microscopy. In *A Handbook of Determinative Methods in Clay Minerals*; Wilson, M.J., Ed.; Blackie & Son Ltd.: New York, NY, USA, 1987; pp. 209–247.
27. Ravisankar, R.; Kiruba, S.; Shamira, C.; Naseerutheen, A.; Balaji, P.D.; Seran, M. Spectroscopic techniques applied to characterization of recently excavated ancient potteries from Thruverkadu Tamilandu, India. *Microchem. J.* **2011**, *99*, 370–375. [[CrossRef](#)]
28. Papachristodoulou, C.; Oikonomou, A.; Ioannides, K.; Gravani, K. A study of ancient pottery by means of X-ray fluorescence spectroscopy multivariate statistics and mineralogical analysis. *Anal. Chim. Acta* **2006**, *573–574*, 347–353. [[CrossRef](#)]
29. Nodari, L.; Marcuz, E.; Maritan, L.; Mazzoli, C.; Russo, U. Hematite nucleation and growth in the firing of carbonate-rich clay for pottery production. *J. Eur. Ceram. Soc.* **2007**, *27*, 4665–4673. [[CrossRef](#)]
30. Ravisankar, R.; Kiruba, S.; Eswaran, P.; Senthilkumar, G.; Chandrasekaran, A. Mineralogical Characterization Studies of Ancient Potteries of Tamilnadu, India by FT-IR Spectroscopic Technique. *J. Chem.* **2010**, *7*, S185–S190. [[CrossRef](#)]
31. Ravisankar, R.; Kiruba, S.; Chandrasekaran, A.; Senthilkumar, G.; Maheswaran, C. Analysis on ancient potteries of Tamilandu, India by spectroscopic techniques. *Indian J. Sci. Technol.* **2010**, *3*, 858–862. [[CrossRef](#)]
32. Vasilache, V.; Kavruk, V.; Tencariu, F.A. OM, SEM-EDX, and micro-FTIR analysis of the Bronze Age pottery from the Băile Figa salt production site (Transylvania, Romania). *Microsc. Res. Tech.* **2020**, *83*, 604–617. [[CrossRef](#)]
33. Duma, G. Phosphate Content of Ancient Pots as Indication of Use. *Curr. Anthropol.* **1972**, *13*, 127–130. [[CrossRef](#)]
34. Béarat, H.; Dufournier, D. Quelques expériences sur la fixation du phosphore par les céramiques. *ArchéoSci. Rev. D'Archéométrie* **1994**, *18*, 65–73. [[CrossRef](#)]
35. Freudiger-Bonzon, J. Archaeometrical Study (Petrography, Mineralogy and Chemistry) of Neolithic Ceramics from Ar-bon Bliche 3 (Canton of Thurgau, Switzerland). Ph.D. Thesis, Faculté des Sciences, Université de Freiburg, Freiburg, Switzerland, 2005.
36. Santos Rodrigues, S.F.; Lima da Costa, M. Phosphorus in archaeological ceramics as evidence of the use of pots for cooking food. *Appl. Clay Sci.* **2016**, *123*, 224–231. [[CrossRef](#)]
37. Karapukaitytė, A.; Pakutinskienė, I.; Tautkus, S.; Kareiva, A. SEM and EDX characterization of ancient pottery. *Lith. J. Phys.* **2006**, *46*, 383–388. [[CrossRef](#)]
38. Aroke, U.O.; Abdulkarim, A.; Ogubunka, R.O. Fourier-transform Infrared Characterization of Kaolin, Granite, Bentonite and Barite. *ATBU J. Environ. Technol.* **2013**, *6*, 42–53.
39. Forte, V.; Cesaro, S.N.; Medeghini, L. Cooking traces on Copper Age pottery from central Italy: An integrated approach comparing use wear analysis, spectroscopic analysis and experimental archaeology. *J. Archeol. Sci. Rep.* **2018**, *18*, 121–138. [[CrossRef](#)]
40. Frost, R.L.; Vassallo, A.M. The dehydroxylation of the kaolinite clay minerals using infrared emission spectroscopy. *Clays Clay Miner.* **1996**, *44*, 635–651. [[CrossRef](#)]
41. Damjanović, L.; Holclajtner-Antunović, I.; Mioč, U.B.; Bikić, V.; Milovanović, D.; Radosavljević Evans, I. Archaeometric study of medieval pottery excavated at Stari (old) Ras, Serbia. *J. Archaeol. Sci.* **2011**, *38*, 818–828. [[CrossRef](#)]
42. Manoharan, S.P.; Venkatachalapathy, R.; Vasanthi, S.; Dhanopandian, S.; Veeramuthu, K. Spectroscopic and rock magnetic studies on some ancient Indian pottery samples. *Egypt. J. Basic Appl. Sci.* **2015**, *2*, 39–49. [[CrossRef](#)]
43. Oancea, A.V.; Bodi, G.; Nica, V.; Ursu, L.E.; Drobotă, M.; Cotofana, C.; Vasiliu, A.L.; Simionescu, B.C.; Olaru, M. Multi-analytical characterization of Cucuteni pottery. *J. Eur. Ceram. Soc.* **2017**, *37*, 5079–5098. [[CrossRef](#)]
44. Costa, T.G.; Correia, M.D.d.M.; Reis, L.B.; dos Santos, S.S.; Machado, J.S.; Bueno, L.; da Silva Müller, I. Spectroscopic characterization of recently excavated archaeological potsherds of Taquaea/Itararé tradition from Tobias Wagner site (Santa Catarina-Brazil). *J. Archeol. Sci. Rep.* **2017**, *12*, 561–568. [[CrossRef](#)]

45. Tironi, A.; Trezza, M.A.; Irassar, E.F.; Scian, A.N. Thermal treatment of kaolin: Effect on the pozzolanic activity. *Procedia Mater. Sci.* **2012**, *1*, 343–350. [[CrossRef](#)]
46. Chen, Y.; Zou, C.; Mastalerz, M.; Hu, S.; Gasaway, C.; Tao, X. Applications of Micro-Fourier Transform Infrared Spectroscopy (FTIR) in the Geological Sciences—A Review. *Int. J. Mol. Sci.* **2015**, *16*, 30223–30250. [[CrossRef](#)]
47. Velraj, G.; Janaki, K.; Mustafa, A.M.; Palanivel, R. Estimation of firing temperatures of some archaeological pottery sherds excavated recently in Tamilandu, India. *Spectrochim. Acta A* **2009**, *72*, 730–733. [[CrossRef](#)]
48. Palanivel, R.; Kumar, U.R. Thermal and spectroscopic analysis of ancient potteries. *Rom. J. Phys.* **2011**, *56*, 195–208.
49. Velraj, G.; Tamilarasu, S.; Ramaya, R. FTIR, XRD and SEM-EDS studies of archaeological pottery samples from recently excavated site in Tamil Nadu, India. *Mater. Today* **2015**, *2*, 934–942. [[CrossRef](#)]
50. Berzina-Cimdina, L.; Borodajenko, N. Research of Calcium Phosphates Using Fourier Transform Infrared Spectroscopy. In *Infrared Spectroscopy: Materials Science, Engineering and Technology*; Theopantides, T., Ed.; IntechOpen: London, UK, 2012; pp. 123–148.
51. Miller, F.A.; Wilkins, C.H. Infrared Spectra and Characteristic Frequencies of Inorganic Ions. Their Use in Qualitative Analysis. *Anal. Chem.* **1952**, *24*, 1253–1294. [[CrossRef](#)]
52. Kumar, R.S.; Rajkumar, P. Characterization of minerals in air dust particles in the state of Tamilandu, India through FTIR Spectroscopy. *Infrared Phys. Technol.* **2014**, *67*, 30–41. [[CrossRef](#)]
53. Gasaway, C.; Mastalerz, M.; Krause, F.; Clarkson, C.; Debuhr, C. Applicability of Micro-FTIR in Detecting Shale Heterogeneity. *Microscopy* **2017**, *265*, 60–72. [[CrossRef](#)] [[PubMed](#)]
54. Niculae, M.D. Sistem Integrat Pentru Stabilirea Identității Probelor Ceramice. Ph.D. Thesis, “Dunarea de Jos” University, Galati, Romania, 2011.
55. Barilaro, D.; Barone, G.; Crupi, V.; Majolino, D.; Mazzoleni, P.; Tigano, G.; Venuti, V. FT-IR absorbance spectroscopy to study Sicilian “proto-majolica” pottery. *Vib. Spectrosc.* **2008**, *48*, 269–275. [[CrossRef](#)]
56. Akyuza, S.; Guliyev, F.; Celik, S.; Ozel, A.E.; Alakbarov, V. Investigations of the Neolithic potteries of 6th millennium BC from Goytepe-Azerbaijan by vibrational spectroscopy and chemometric techniques. *Vib. Spectrosc.* **2019**, *105*, 102980. [[CrossRef](#)]
57. Stevenson, C.M.; Gurnick, M. Structural collapse in kaolinite, montmorillonite and illite clay and its role in the ceramic rehydroxylation dating of low-fired earthenware. *J. Archaeol. Sci.* **2016**, *69*, 54–63. [[CrossRef](#)]
58. Hofmeister, A.M.; Bowey, J.E. Quantitative infrared spectra of hydrosilicates and related minerals. *Mon. Not. R. Astron. Soc.* **2006**, *367*, 577–591. [[CrossRef](#)]

**Disclaimer/Publisher’s Note:** The statements, opinions and data contained in all publications are solely those of the individual author(s) and contributor(s) and not of MDPI and/or the editor(s). MDPI and/or the editor(s) disclaim responsibility for any injury to people or property resulting from any ideas, methods, instructions or products referred to in the content.